

AD-A171 895

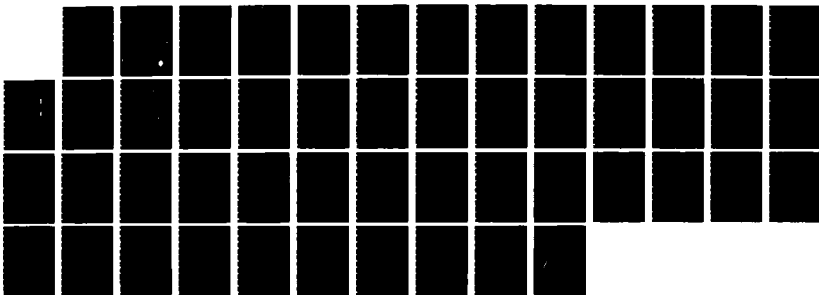
ACCURATE DETERMINATION OF THE PERMITTIVITY AND
CONDUCTIVITY OF BIOLOGICAL (U) KING'S COLL LONDON
(ENGLAND) DEPT OF PHYSICS E H GRANT APR 86
USAFSAM-TR-84-33 AFOSR-81-0097

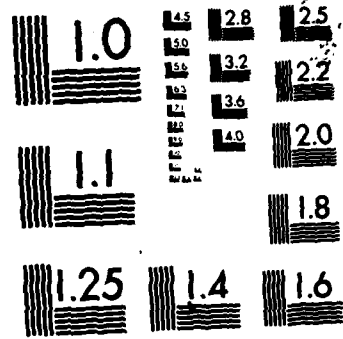
1/1

UNCLASSIFIED

F/G 6/3

NL





MICROCOPY RESOLUTION TEST CHART
NATIONAL BUREAU OF STANDARDS-1963-A

12

USAFSAM-TR-84-33

ACCURATE DETERMINATION OF THE PERMITTIVITY AND CONDUCTIVITY OF BIOLOGICAL TISSUE AT CENTIMETRE AND MILLIMETRE WAVELENGTHS

E.H. Grant, Ph.D., F.R.S.

**Physics Department
King's College, London
Strand, London WC2R 2LS, UK**

April 1986

Final Report for Period 1 February 1981 - 30 April 1984

**DTIC
ELECTE
SEP 16 1986**
S
B

Approved for public release; distribution is unlimited.

Prepared for

**USAF SCHOOL OF AEROSPACE MEDICINE
Aerospace Medical Division (AFSC)
Brooks Air Force Base, TX 78235-5301**

**European Office of Aerospace Research
and Development (LSB)
223-231 Old Marylebone Road
London NW1 5TH, UK**



AD-A171 895

DTIC FILE COPY

86 9 16 066

NOTICES

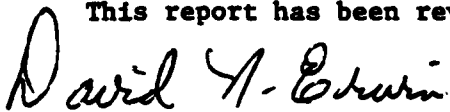
This final report was submitted by the Physics Department, King's College, London, Strand, London WC2R 2LS, United Kingdom, under contract AFOSR-81-0097, job order 2312-V7-07, with the USAF School of Aerospace Medicine, Aerospace Medical Division, AFSC, Brooks Air Force Base, Texas. Dr. David N. Erwin (USAFSAM/RZP) was the Laboratory Project Scientist-in-Charge.

When Government drawings, specifications, or other data are used for any purpose other than in connection with a definitely Government-related procurement, the United States Government incurs no responsibility nor any obligation whatsoever. The fact that the Government may have formulated or in any way supplied the said drawings, specifications, or other data, is not to be regarded by implication, or otherwise in any manner construed, as licensing the holder or any other person or corporation; or as conveying any rights or permission to manufacture, use, or sell any patented invention that may in any way be related thereto.

The animals involved in this study were procured, maintained, and used in accordance with the Animal Welfare Act and the "Guide for the Care and Use of Laboratory Animals" prepared by the Institute of Laboratory Animal Resources - National Research Council.

The Office of Public Affairs has reviewed this report, and it is releasable to the National Technical Information Service where it will be available to the general public, including foreign nationals.

This report has been reviewed and is approved for publication.


DAVID N. ERWIN, Ph.D.
Project Scientist


JOHN C. MITCHELL, B.S.
Supervisor


JEFFREY G. DAVIS, Colonel, USAF, MC
Commander

AD-A171995

REPORT DOCUMENTATION PAGE

1a. REPORT SECURITY CLASSIFICATION UNCLASSIFIED		1b. RESTRICTIVE MARKINGS	
2a. SECURITY CLASSIFICATION AUTHORITY		3. DISTRIBUTION / AVAILABILITY OF REPORT Approved for public release; distribution is unlimited.	
2b. DECLASSIFICATION / DOWNGRADING SCHEDULE		4. PERFORMING ORGANIZATION REPORT NUMBER(S)	
4. PERFORMING ORGANIZATION REPORT NUMBER(S)		5. MONITORING ORGANIZATION REPORT NUMBER(S) USAFSAM-TR-84-33	
6a. NAME OF PERFORMING ORGANIZATION Physics Department King's College, London	6b. OFFICE SYMBOL (if applicable)	7a. NAME OF MONITORING ORGANIZATION European Office of Aerospace Research and Development (LSB)	
6c. ADDRESS (City, State, and ZIP Code) King's College, Strand, London WC2R 2LS, UK		7b. ADDRESS (City, State, and ZIP Code) 223-231 Old Marylebone Road London NW1 5TH, UK	
8a. NAME OF FUNDING / SPONSORING ORGANIZATION USAF School of Aerospace Medicine	8b. OFFICE SYMBOL (if applicable) USAFSAM/RZP	9. PROCUREMENT INSTRUMENT IDENTIFICATION NUMBER Grant AFOSR-81-0097	
8c. ADDRESS (City, State, and ZIP Code) Aerospace Medical Division (AFSC) Brooks Air Force Base, TX 78235-5301		10. SOURCE OF FUNDING NUMBERS	
		PROGRAM ELEMENT NO. 61102F	PROJECT NO. 2312
		TASK NO. V7	WORK UNIT ACCESSION NO. 07
11. TITLE (Include Security Classification) ACCURATE DETERMINATION OF THE PERMITTIVITY AND CONDUCTIVITY OF BIOLOGICAL TISSUE AT CENTIMETRE AND MILLIMETRE WAVELENGTHS			
12. PERSONAL AUTHOR(S) Grant, E.H.			
13a. TYPE OF REPORT Final report	13b. TIME COVERED FROM 1 Feb 81 to 30 Apr 81	14. DATE OF REPORT (Year, Month, Day) 1986 April	15. PAGE COUNT 50
16. SUPPLEMENTARY NOTATION			
17. COSATI CODES		18. SUBJECT TERMS (Continue on reverse if necessary and identify by block number)	
FIELD	GROUP	SUB-GROUP	
06	18		
20	14		
		Microwave measuring technique	
		Permittivity	
		Conductivity	
		Brain tissue	
		Lens material	
		Water content	
19. ABSTRACT (Continue on reverse if necessary and identify by block number)			
<p>An apparatus has been set up and a technique devised to determine the complex permittivity of solid biological tissue in the frequency range 1-18 GHz. The uncertainties in the measured values of permittivity and conductivity were 1% and 2% respectively.</p> <p>Comparative dielectric measurements performed on brain tissue and lens material showed that the latter had a much higher proportion of its water content affected by the presence of biological macromolecules.</p>			
20. DISTRIBUTION / AVAILABILITY OF ABSTRACT <input checked="" type="checkbox"/> UNCLASSIFIED/UNLIMITED <input type="checkbox"/> SAME AS RPT. <input type="checkbox"/> DTIC USERS		21. ABSTRACT SECURITY CLASSIFICATION Unclassified	
22a. NAME OF RESPONSIBLE INDIVIDUAL Dr. David N. Erwin		22b. TELEPHONE (Include Area Code) (512) 536-3582	22c. OFFICE SYMBOL USAFSAM/RZP

CONTENTS

	<u>Page</u>
INTRODUCTION	1
BACKGROUND TO THE EXPERIMENTAL SYSTEM	2
THEORY	4
EXPERIMENTAL METHOD	6
RESULTS FOR RABBIT BRAIN	11
Electrical Properties of Mature Rabbit Brain	11
Electrical Properties of Rat and Mouse Brain	21
Electrical Properties of Developing Rabbit Brain	21
Bound Water Estimation	29
RESULTS FOR RABBIT LENS	32
CONCLUSIONS	42
REFERENCES	43

List of Illustrations

Figure

1	A dielectric sample of thickness d_s enclosed in a coaxial line, held in position by a PTFE sleeve of thickness d_p , and terminated by a short circuit	4
2	Diagram of coaxial-line system	8
3	Inner and outer conductor sections of the cell	9
4	Sample-thickness setting	10
5	The permittivity of rabbit brain at 37°C	12
6	The conductivity of rabbit brain at 37°C	13
7	The permittivity of rabbit brain at 20°C	17
8	The conductivity of rabbit brain at 20°C	18
9	The permittivity of macerated brain tissue, showing various species at 37°C	22
10	The conductivity of macerated brain tissue, showing various species at 37°C	23
11	The permittivity of developing rabbit brain at 37°C	25
12	The conductivity of developing rabbit brain at 37°C	26
13	Microwave static permittivity (ϵ_s) v. age, for developing rabbit brain	27
14	The decrease in microwave static permittivity (ϵ_s) v. decrease in water content during rabbit brain development.	28

		<u>Page</u>
15	The permittivity of rabbit lens at 37°C	33
16	The conductivity of rabbit lens at 37°C	34
17	The permittivity of rabbit lens at 20°C	36
18	The conductivity of rabbit lens at 20°C	37

List of Tables

Table

1	Grey matter (rabbit) at 37°C	15
2	White matter (rabbit) at 37°C	15
3	Macerated brain (rabbit) at 37°C	16
4	Grey matter (rabbit) at 20°C	19
5	White matter (rabbit) at 20°C	19
6	Macerated brain (rabbit) at 20°C	20
7	Developing rabbit brain at 37°C	24
8	Bound water in adult rabbit brain	30
9	Bound water in brain of different species	30
10	Bound water in developing rabbit brain.	31
11	Lens cortex (rabbit) at 37°C	35
12	Lens nucleus (rabbit) at 37°C	38
13	Lens cortex (rabbit) at 20°C	39
14	Lens nucleus (rabbit) at 20°C	40
15	Bound water in rabbit lens	41

ACCURATE DETERMINATION OF THE PERMITTIVITY AND CONDUCTIVITY OF
BIOLOGICAL TISSUE AT CENTIMETRE AND MILLIMETRE WAVELENGTHS

INTRODUCTION

The purpose of this research was to obtain accurate values of the electrical parameters of tissues in the microwave region. This report describes the coaxial-line apparatus that was developed to enable the permittivity, ϵ' , and conductivity, σ , to be measured from 1 to 18 GHz. Data were obtained for the brain and eyelens, mainly of the rabbit although some brain data were also acquired for mouse and rat. The results provided useful information in their own right and have also been analysed to obtain a greater insight into the nature and structure of water in such systems.

The research grant gave financial support to a postgraduate worker (M.C. Steel) who, on the basis of the work carried out, was awarded the Ph.D. degree by the University of London. The thesis, a copy of which has been sent to the Air Force Office of Scientific Research, gives a much more detailed account of the work than is possible in this report.



DTIC
ELECTE
SEP 16 1986
S B

Accession For	
DATE	<input checked="" type="checkbox"/>
BY	
CLASS	
INDEX	
FILE	
Dist	A-1

BACKGROUND TO THE EXPERIMENTAL SYSTEM

Within recent years various papers have appeared in the literature that describe methods for measuring the complex permittivity of solid tissues in both the time and frequency domains; for example, Foster et al. (1979), Schepps and Foster (1980), Burdette et al. (1980), and Stuchly et al. (1981, 1982a, 1982b). Although most of the measuring systems have been broad band and some enable the rapid acquisition of data, the basic experimental techniques are not as accurate as the established frequency domain methods for measuring the complex permittivity of liquids (Sheppard and Grant 1972; Sheppard 1972; Grant, Sheppard, and South 1978, and Szwarnowski and Sheppard 1977).

The objective of this study was to devise a technique suitable for solid tissues whose accuracy would approach that of the traditional techniques used for liquids. While such a method could not make rapid measurements over a broad frequency band, the objective of this work was to make accurate spot measurements within the frequency band of 1-18 GHz, i.e., accuracy rather than speed. However, a single measurement could be obtained in less than 15 min, including loading of the sample holder and attainment of thermal stability.

The technique used in our laboratory to measure precisely the complex permittivity of a liquid up to 4 GHz (Sheppard and Grant 1972, Sheppard 1972) involves moving a probe through the liquid. Between 2 and 18 GHz a different method was used involving a cell with a movable short circuit, which enables the path length through the liquid to be varied (Nightingale et al. 1981). Clearly neither of these techniques would be suitable for solid tissues.

One standard method for measuring the permittivity and conductivity of liquids and solids has been described by Roberts and Von Hippel (1946). Their technique was believed to be a sound method for measuring these dielectric parameters; and if, with appropriate modification, it were set up using modern precision microwave components coupled with an on-line computer for data acquisition and analysis, the required accuracy would be obtained.

In particular it was necessary to move away from the idea, inherent in the original Roberts and Von Hippel method, of measuring only a standard wave ratio. In the present system the entire profile of the reflected wave is recorded on a floppy disc and then analysed by a microcomputer. This is advantageous when the minima and maxima are poorly defined and it also allows many more data points to be taken.

THEORY

The experimental cell (details of which are given in the next section) consists of a PTFE window of thickness d_p , followed by a tissue sample of thickness d_s , terminated with a short circuit (Fig. 1). At distance x in front of a PTFE-air interface, the power reflection profile is given by

$$P(x) = |A|^2 \cdot |\exp(-\gamma_a x) + \rho'_{12} \exp(\gamma_a x)|^2 \quad (1)$$

where γ_a is the propagation constant of an air-filled line, A is a constant, and ρ'_{12} is the total reflection coefficient of the system.

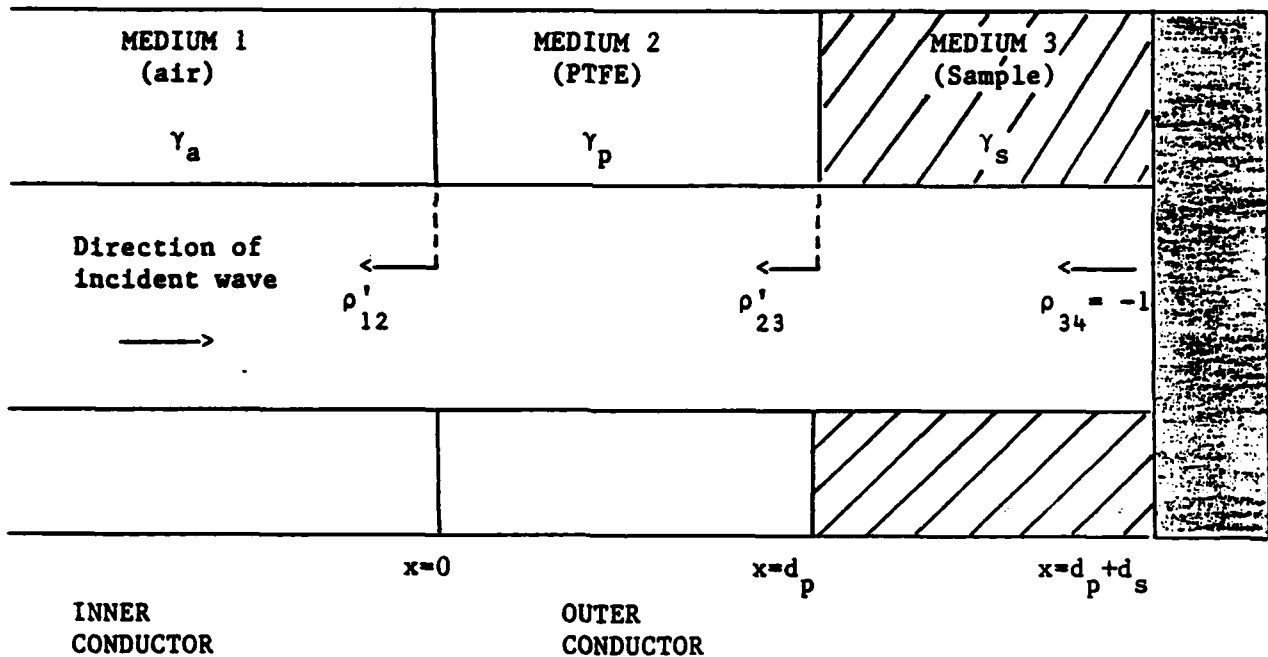


Figure 1. A dielectric sample of thickness d_s enclosed in a coaxial line, held in position by a PTFE sleeve of thickness d_p , and terminated by a short circuit.

Considering the multiple reflections between the various interfaces of the system, it can be shown that

$$\rho'_{12} = \frac{\rho_{12} + \rho'_{23} \exp(-2\gamma_p d_p)}{1 + \rho_{12} \rho'_{23} \exp(-2\gamma_p d_p)} \quad (2)$$

and

$$\rho'_{23} = \frac{\rho_{23} - \exp(-2\gamma_s d_s)}{1 - \rho_{23} \exp(-2\gamma_s d_s)} \quad (3)$$

where γ_p and γ_s are the propagation constants of PTFE and sample respectively.

Now

$$\rho_{12} = \frac{\gamma_a - \gamma_p}{\gamma_a + \gamma_p} \quad (4)$$

$$\rho_{23} = \frac{\gamma_p - \gamma_s}{\gamma_p + \gamma_s} \quad (5)$$

and

$$\gamma_s = \frac{2\pi}{\lambda_a} (-\epsilon)^{1/2} \quad (6)$$

where λ_a is the free space wavelength and ϵ is the complex relative permittivity of the sample. Thus the power reflection profile, $P(x)$, contains the parameter of interest, namely ϵ , within ρ'_{12} . Hence, by observing experimentally $P(x)$ as a function of x , the complex permittivity, ϵ , can be obtained from the usual computer least-squares curve-fitting technique (Sheppard 1973). In particular the parameters fitted are ϵ ($\epsilon = \epsilon' - j\epsilon''$) and A ; λ_a is known for air and γ_p is measured experimentally.

EXPERIMENTAL METHOD

The microwave circuit (Fig. 2) consists of a Hewlett-Packard slotted line with the experimental cell connected directly to it. The power is supplied by a General Radio oscillator between 1.7 and 4 GHz, a Varian Klystron over the range 7.5-8.5 GHz, and a series of Plessey Gunn diodes at spot frequencies between 9.5 and 18 GHz. The microwave signal passes through an isolator and is then divided by a probe coupler so that part of the signal can be fed to a digital frequency counter. After more isolators the signal is modulated with a PIN diode and then fed through the slotted line to the experimental cell. The modulated output from the standing wave detector is fed via a lock-in amplifier to a digital voltmeter, which is interfaced via an IEEE 488 bus to a Research Machines 380Z microcomputer.

The experimental cell (Fig. 3) consists of a precision 7-mm Amphenol air line which is surrounded with a water jacket for thermostating purposes. A PTFE sleeve is followed by a precise gap for the tissue sample, which is terminated by a short circuit that makes direct contact with the sample. The PTFE is accurately machined so that, although it fits tightly onto the inner conductor, it can, with a little pressure, be moved inside the outer conductor. The short circuit can be unscrewed from the inner conductor so that the tissue can be easily loaded into the cell.

Although this cell is similar to that used for our time-domain spectrometer (Dawkins et al. 1979), there are two main differences; this inner conductor keeps a constant dimension throughout the cell, and the short circuit is an integral part of the cell rather than being placed a few centimetres behind it.

Sample thickness must be accurately set; the method for achieving this is shown in Fig. 4. A mild steel disc, machined accurately to the required thickness, is placed onto the inner conductor against the short circuit. The PTFE can be pushed against the disc and the short circuit, then removed so that the disc can be released and the tissue packed around the inner conductor. The short circuit and its thread are accurately made so that

when the short circuit is replaced, the tissue thickness equals that of the disc.

It is necessary to know the permittivity of the PTFE, and the samples used were measured and found to be 2.035 ± 0.002 . The cell was fully tested on both water and tissue samples before this investigation was undertaken. The results of the tests and a consideration of the likely errors were reported by Steel et al. (1984).

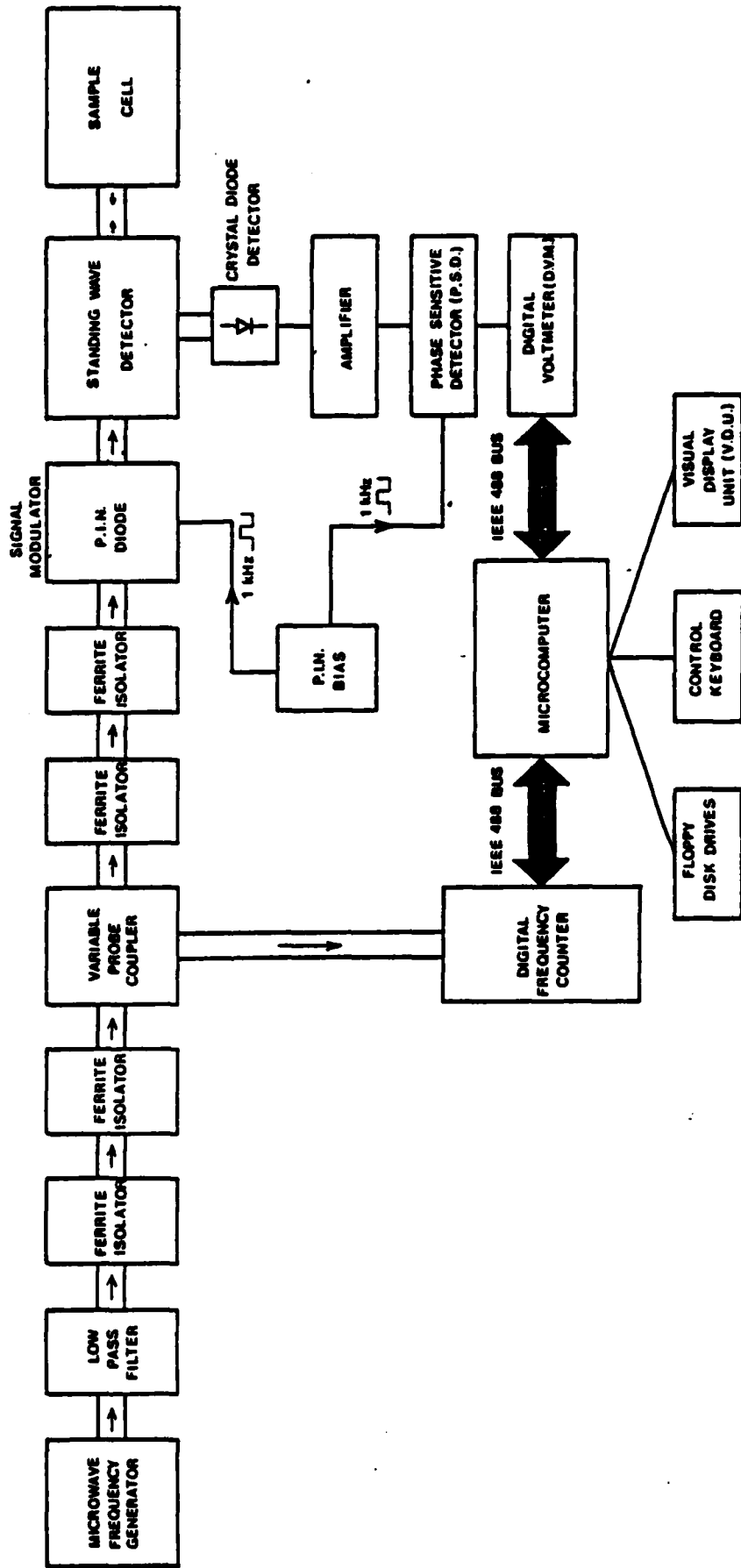
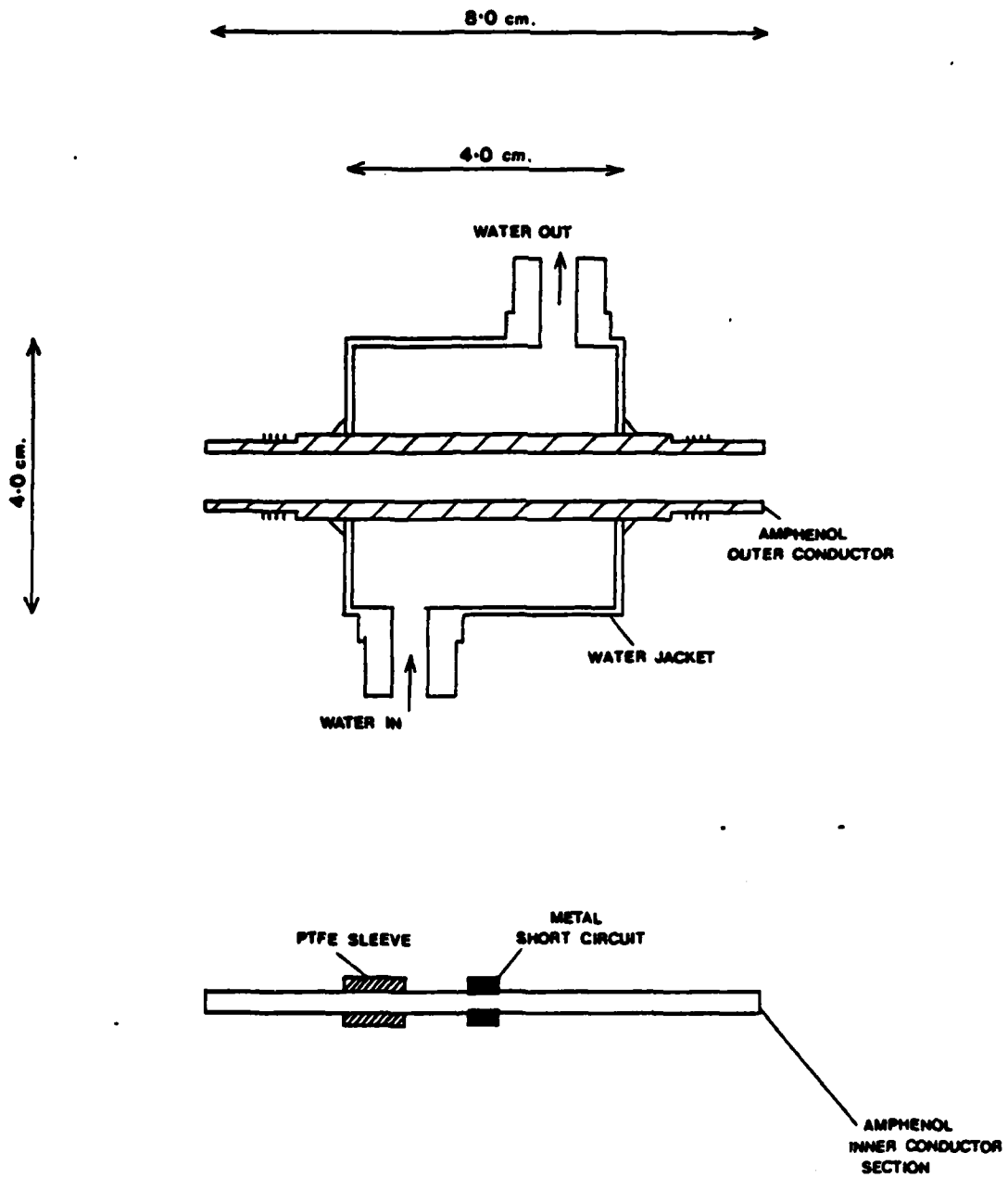


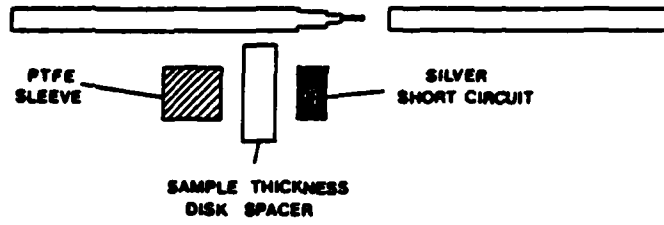
Figure 2. Diagram of coaxial-line system.



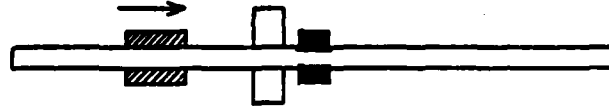
(SCALE 1:1)

Figure 3. Inner and outer conductor sections of the cell.

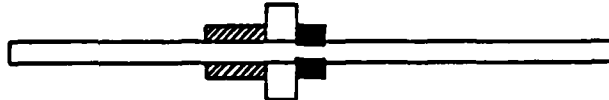
STAGE 1



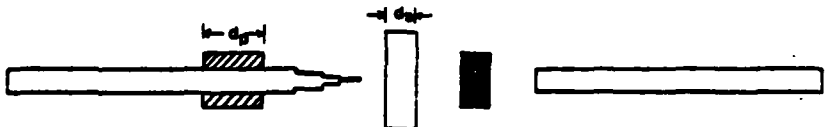
STAGE 2



STAGE 3



STAGE 4



STAGE 5

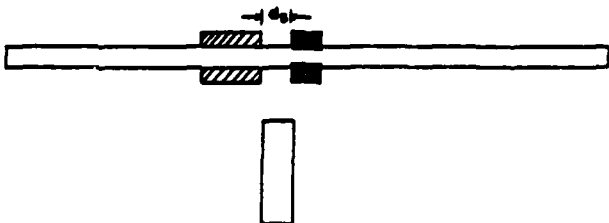


Figure 4. Sample-thickness setting.

RESULTS FOR RABBIT BRAIN

The following sections present data on the electrical properties of mature rabbit brain, developing rabbit brain, and rabbit eye lens.

Electrical Properties of Mature Rabbit Brain

For the initial investigation Dutch pigmented rabbits about 8 months old were used. After a lethal injection of pentobarbitonesodium, the whole brain was excised and the grey and white matter were separated so that they could be measured separately. In addition some macerated whole-brain samples were prepared. Full details of the care required in handling and loading the tissue were presented by Steel (1984). Nearly all measurements were performed within 8 h of the sacrifice of the animal; however, in an experiment in which samples were measured quickly after sacrifice and then remeasured over a 24-h period, no significant variations could be found.

The permittivity and conductivity of grey matter, white matter, and macerated rabbit brain at 37°C are shown in Figs. 5 and 6, respectively, over a frequency range of 1-18 GHz. As expected, the results for the macerated brain lie between those for white and grey matter. The data were fitted to the Debye and Cole-Cole models (equations 7 and 8 respectively):

$$\epsilon = \frac{\epsilon_s - \epsilon_\infty}{1 + j f/f_R} + \epsilon_\infty - \frac{j \sigma}{2\pi f \epsilon_0} \quad (7)$$

$$\epsilon = \frac{\epsilon_s - \epsilon_\infty}{1 + (jf/f_R)^{1-\alpha}} + \epsilon_\infty - \frac{j \sigma}{2\pi f \epsilon_0} \quad (8)$$

where α is the Cole-Cole parameter and σ the ionic conductivity.

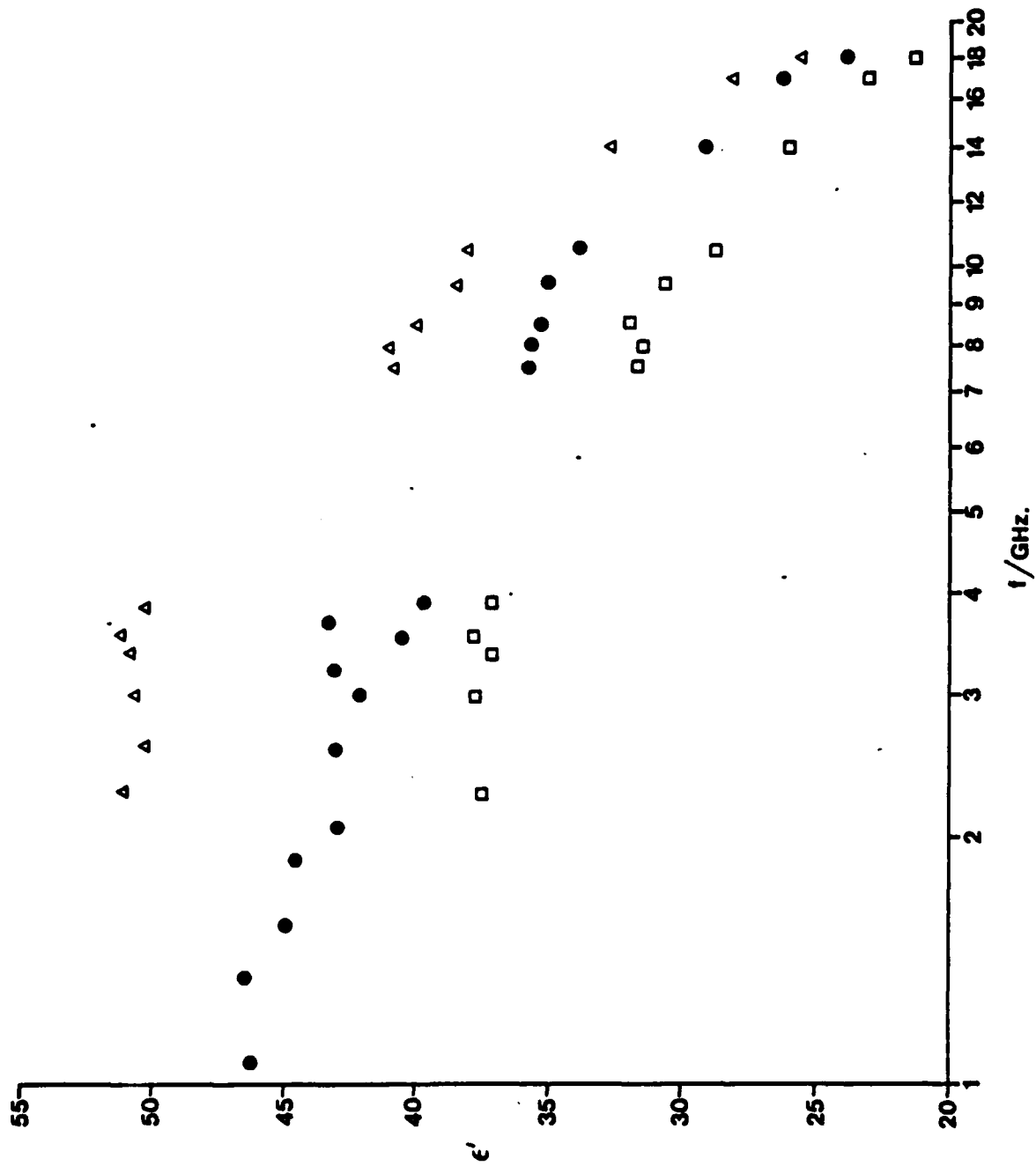


Figure 5. The permittivity of rabbit brain at 37°C.

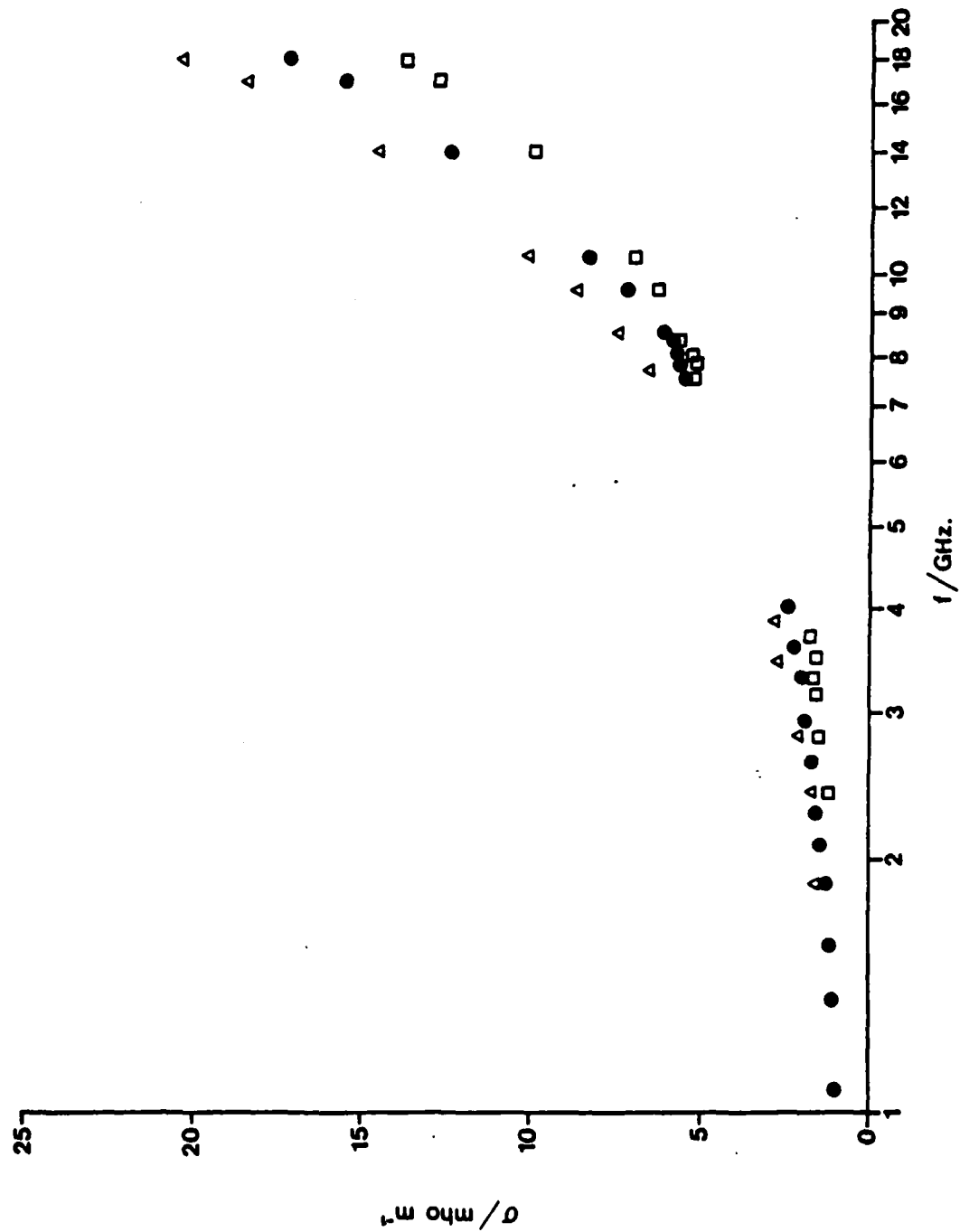


Figure 6. The conductivity of rabbit brain at 37° C.

The results for the grey matter, white matter, and macerated brain are presented in Tables 1, 2, and 3 respectively. For analysis the data have been divided into various frequency regions. The macerated brain could be divided into more regions than either the white or the grey since more data points were available. Table 3 (macerated brain) shows that the Debye model fitted to data over the range 1-4 GHz gives a relaxation frequency of 17.4 ± 2 GHz which is significantly less than the pure water value of 25.4 GHz. However, the Cole-Cole analysis gives a better fit, with an α of 0.33 ± 0.13 , but the relaxation frequency is now not shifted from the pure water value. In previous work Nightingale et al. (1983) reported a Cole-Cole α ranging from 0.33 ± 0.16 for brain cerebrum to 0.55 ± 0.17 for brain stem.

In the analysis of the high frequency part of the data (7.5-18 GHz) (Table 3), the Cole-Cole α at 0.04 ± 0.04 is small and not significantly different from zero; hence, the data can be represented by the Debye model. The other ranges of the data shown in Table 3 tend to lie within the extreme values considered. Table 1 shows that the grey matter is similar in behaviour to the macerated brain. The white matter, however, has a significant $\alpha = 0.18 \pm 0.11$ for the range 7.5 to 18 GHz (Table 2).

The above work was repeated at 20°C , where the relaxation frequency of pure water is 16.8 GHz and thus within the range of the apparatus. The permittivity and conductivity data are shown in Figs. 7 and 8 and the analysis in Tables 4, 5, and 6. Again concentrating on the macerated brain, α is only significantly different from 0 when the low frequency data are analysed; and a Single Debye model gives a reduced relaxation frequency (14 ± 2 GHz). Also, as at 37°C , the behaviour of grey matter is similar to macerated brain, whereas the white matter gives an α of 0.12 ± 0.09 for the high frequency data.

TABLE 1. GREY MATTER (RABBIT) AT 37°C

Range/GHz	N ^a	ϵ_s	f_R /GHz	α	σ_1 /mho m ⁻¹	RMSE
1.9-18	24	47.1 (0.7) ^b	23.8 (1.2)	-	1.21 (0.14)	0.968
		49.2 (0.9)	23.6 (0.9)	0.09 (0.03)	1.09 (0.10)	0.580
1.9-10.5	18	47.6 (0.7)	22.4 (1.6)	-	1.16 (0.14)	0.858
		49.4 (1.3)	23.1 (1.5)	0.10 (0.06)	1.07 (0.13)	0.640
7.6-18	14	45.0 (0.7)	26.3 (1.3)	-	1.91 (0.43)	0.409
		47.2 (1.7)	25.2 (1.4)	0.05 (0.04)	1.57 (0.41)	0.293

^aThe number of real and imaginary data points used in the analysis.

^bThe errors are the 95% confidence intervals.

$$(\epsilon_\infty = 5.1)$$

TABLE 2. WHITE MATTER (RABBIT) AT 37°C

Range/GHz	N ^a	ϵ_s	f_R /GHz	α	σ_1 /mho m ⁻¹	RMSE
2.4-18	30	35.3 (0.6) ^b	24.6 (1.9)	-	0.84 (0.20)	1.012
		36.8 (1.3)	24.6 (2.0)	0.09 (0.07)	0.75 (0.19)	0.829
2.4-10.5	24	35.8 (0.6)	22.1 (1.9)	-	0.73 (0.19)	0.858
		35.3 (1.0)	21.9 (2.1)	0.00 (0.06)	0.76 (0.20)	0.913
7.5-18	18	33.6 (1.0)	30.1 (3.9)	-	2.03 (0.63)	0.814
		38.6 (4.5)	25.7 (6.0)	0.18 (0.11)	1.27 (0.80)	0.608

^aThe number of real and imaginary data points used in the analysis.

^bThe errors are the 95% confidence intervals.

$$(\epsilon_\infty = 5.1)$$

TABLE 3. MACERATED BRAIN (RABBIT) AT 37°C

Range/GHz	N ^a	ϵ_s	f_R /GHz	α	σ_1 /mho m ⁻¹	RMSE
1-18	50	41.6 (0.4) ^b	25.5 (1.3)	-	1.02 (0.06)	0.982
		42.9 (0.7)	26.6 (1.5)	0.10 (0.04)	0.96 (0.06)	0.821
1-10.5	44	41.8 (0.4)	24.3 (1.6)	-	1.00 (0.06)	0.954
		43.3 (0.9)	26.3 (2.1)	0.13 (0.06)	0.94 (0.06)	0.797
1-8	36	41.9 (0.5)	22.2 (2.0)	-	0.97 (0.07)	0.965
		44.1 (1.2)	25.5 (3.0)	0.19 (0.08)	0.88 (0.08)	0.752
1-4	30	42.2 (0.5)	17.4 (2.1)	-	0.87 (0.08)	0.826
		46.6 (2.6)	24.3 (4.2)	0.33 (0.13)	0.76 (0.08)	0.572
3.6-18	28	40.7 (0.3)	27.9 (0.8)	-	1.34 (0.09)	0.363
		41.0 (0.6)	28.0 (0.8)	0.02 (0.03)	1.31 (0.11)	0.349
7.5-18	20	40.6 (0.5)	28.2 (1.4)	-	1.41 (0.30)	0.403
		41.8 (1.4)	27.7 (1.5)	0.04 (0.04)	1.21 (0.35)	0.360

^a The number of real and imaginary data points used in the analysis.

^b The errors are the 95% confidence intervals.

$$(\epsilon_\infty = 5.1)$$

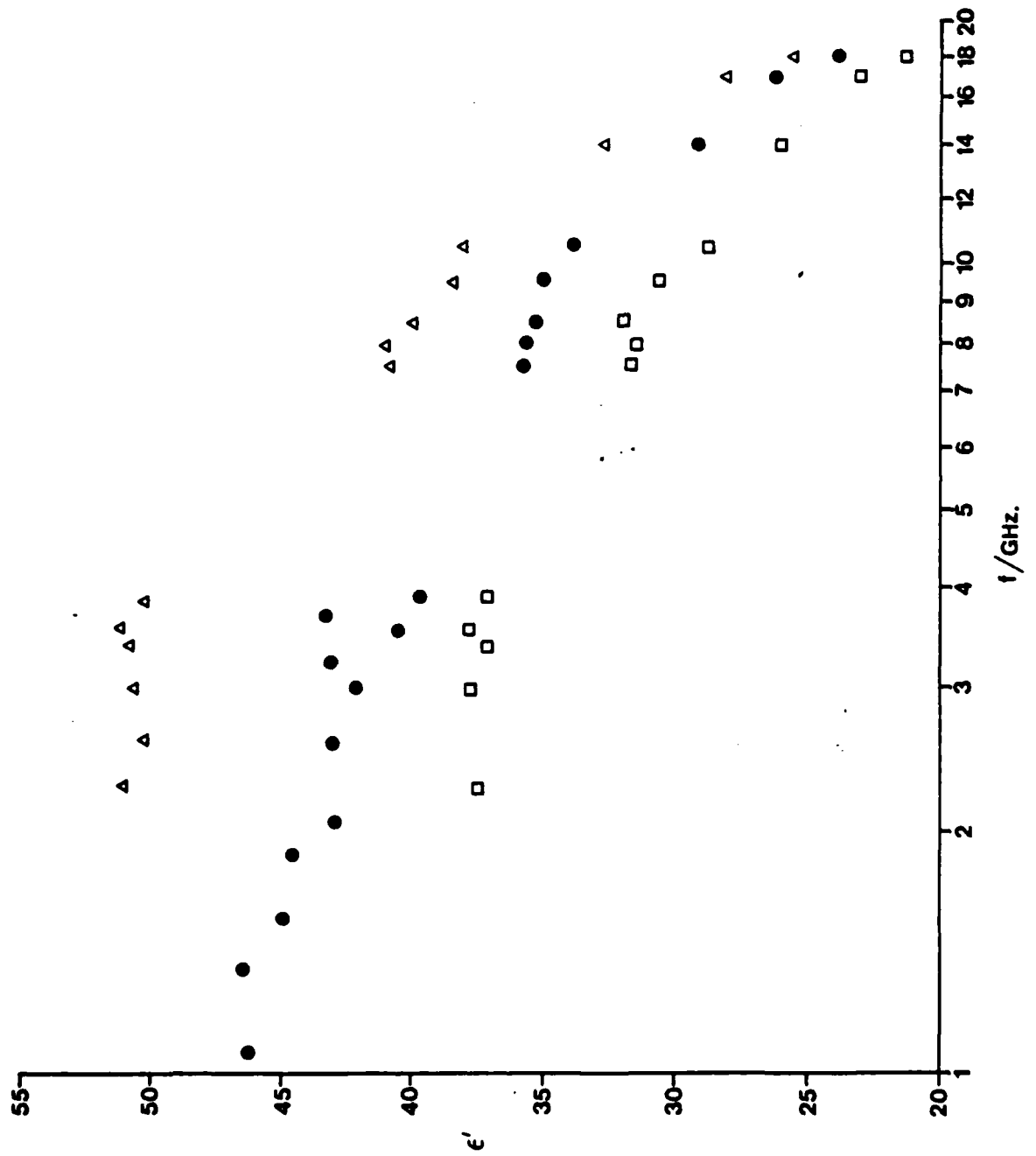


Figure 7. The permittivity of rabbit brain at 20°C.

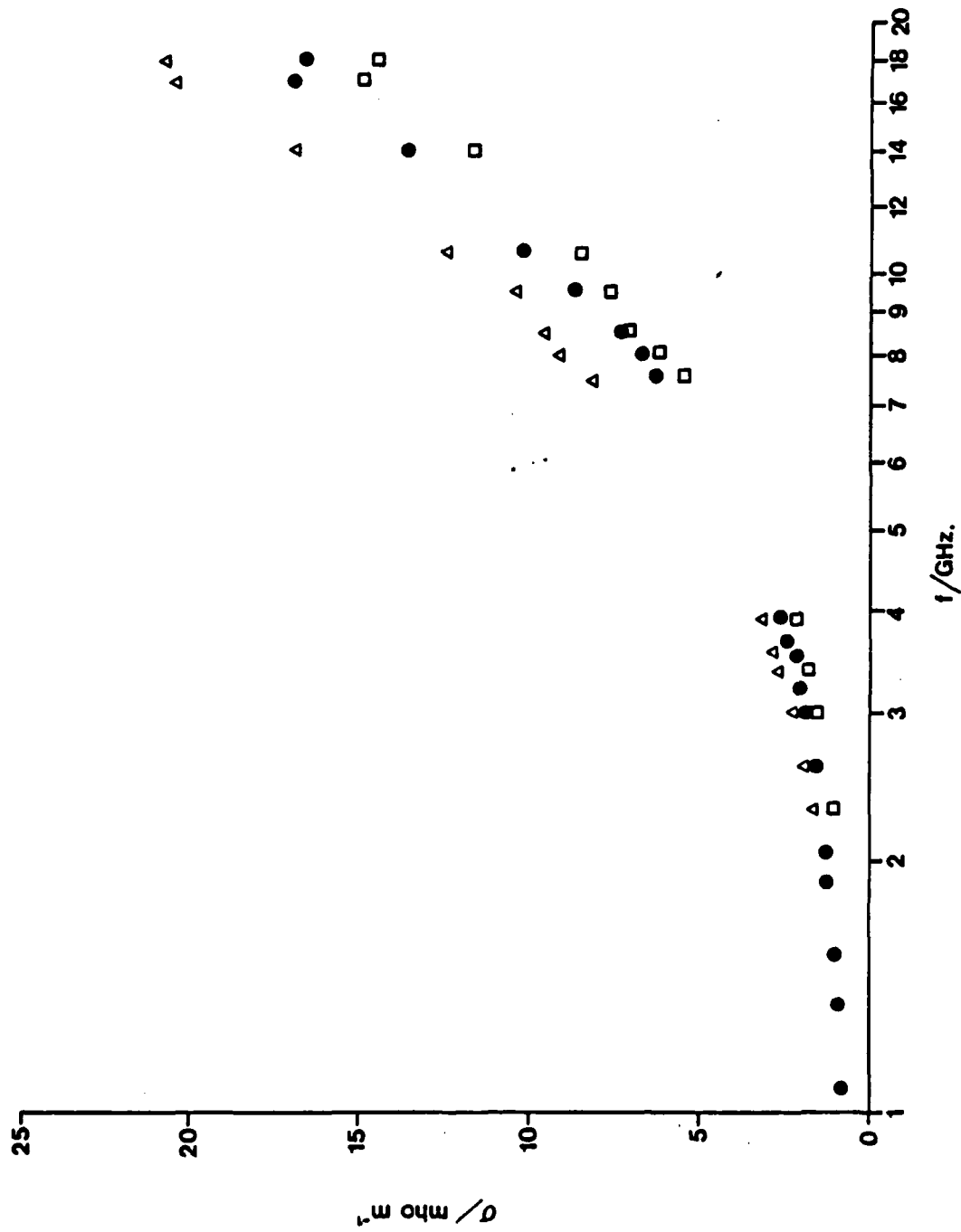


Figure 8. The conductivity of rabbit brain at 20°C.

TABLE 4. GREY MATTER (RABBIT) AT 20°C

Range/GHz	N ^a	ϵ_s	f_R /GHz	α	σ_i /mho m ⁻¹	RMSE
2.3-18	28	51.1 (1.0) ^b	16.1 (0.9)	-	0.82 (0.20)	1.260
		54.8 (1.3)	15.0 (0.7)	0.10 (0.03)	0.58 (0.14)	0.710
2.3-10.5	22	51.6 (0.9)	15.6 (1.0)	-	0.78 (0.19)	1.060
		54.7 (1.7)	15.1 (0.9)	0.10 (0.04)	0.58 (0.16)	0.705
7.5-18	16	46.9 (1.9)	18.5 (1.7)	-	1.86 (0.88)	0.837
		52.0 (5.4)	16.3 (2.7)	0.08 (0.07)	1.14 (1.07)	0.689

^aThe number of real and imaginary data points used in the analysis.

^bThe errors are the 95% confidence intervals.

($\epsilon_\infty = 5.5$)

TABLE 5. WHITE MATTER (RABBIT) AT 20°C

Range/GHz	N ^a	ϵ_s	f_R /GHz	α	σ_i /mho m ⁻¹	RMSE
2.3-18	26	37.7 (0.6) ^b	17.9 (1.0)	-	0.63 (0.03)	0.859
		40.0 (1.0)	17.0 (0.8)	0.10 (0.03)	0.47 (0.11)	0.539
2.3-10.5	20	38.2 (0.5)	16.9 (0.9)	-	0.56 (0.12)	0.571
		39.4 (1.1)	16.7 (0.8)	0.06 (0.05)	0.49 (0.12)	0.479
7.5-18	16	35.6 (1.6)	19.9 (2.2)	-	1.28 (0.77)	0.756
		40.7 (5.3)	16.6 (2.8)	0.12 (0.09)	0.56 (0.96)	0.591

^aThe number of real and imaginary data points used in the analysis.

^bThe errors are the 95% confidence intervals.

($\epsilon_\infty = 5.5$)

TABLE 6. MACERATED BRAIN (RABBIT) AT 20°C

Range/GHz	N ^a	ϵ_s	f_R /GHz	α	σ_1 /mho m ⁻¹	RMSE
1-18	40	43.5 (0.7) ^b	17.5 (1.1)	-	0.73 (0.09)	1.335
		46.1 (0.9)	17.0 (0.9)	0.13 (0.03)	0.62 (0.07)	0.825
1-10.5	34	43.8 (0.7)	16.9 (1.2)	-	0.72 (0.09)	1.219
		46.4 (1.2)	17.1 (1.2)	0.15 (0.05)	0.61 (0.07)	0.847
1-8	28	44.1 (0.7)	15.5 (1.6)	-	0.68 (0.09)	1.194
		47.5 (1.6)	16.5 (1.6)	0.20 (0.07)	0.55 (0.08)	0.773
1-4	24	44.5 (0.7)	14.0 (1.9)	-	0.63 (0.10)	1.054
		48.9 (3.4)	17.0 (3.0)	0.28 (0.15)	0.52 (0.11)	0.805
3.5-18	22	41.5 (1.0)	19.2 (1.3)	-	1.03 (0.30)	1.017
		44.0 (2.1)	18.2 (1.5)	0.08 (0.06)	0.82 (0.29)	0.828
7.6-18	16	40.5 (2.7)	20.0 (2.7)	-	1.24 (0.76)	0.754
		44.6 (4.8)	17.8 (3.1)	0.09 (0.08)	0.65 (0.95)	0.626

^aThe number of real and imaginary data points used in the analysis.

^bThe errors are the 95% confidence intervals.

$$(\epsilon_\infty = 5.5)$$

During the analysis it was necessary to clamp ϵ_∞ at an appropriate value. The precise value is, however, unimportant and may be varied by as much as $\pm 20\%$ without significantly affecting the other parameters.

Foster et al. (1979) concluded that a single relaxation process indistinguishable from that of free water adequately described their data for canine brain at 37°C above a few GHz. This was also later shown for barnacle muscle (Foster et al. 1980), but in both cases data below 5 GHz were still being affected by a relaxation process occurring somewhere between

0.1 and 1 GHz. It seems likely that the large value of α observed in the present work from the low frequency analysis is caused by a mechanism other than bulk water. We believe, however, that above 7.5 GHz the data are sufficiently far away from such processes not to be influenced by them. Certainly the results suggest that the rotational properties of the bulk water in the rabbit brain are similar to those of free water. The small spread of relaxation frequencies evident from the analysis of white matter, however, implies that in this tissue the bulk water is rotationally bound to some degree to the macromolecular structure.

Electrical Properties of Rat and Mouse Brain

To compare the dielectric properties between species, a brief study was made on rats and mice. The brains of five adult brown rats, of the same litter, were pooled and macerated; the animals were 14 weeks old and weighed between 295 and 344 g. The brains of eight mice (strain: BLAB/C) were treated in an identical fashion; the animals were 55 weeks old and weighed between 25 and 30 g. The permittivity and conductivity data are shown in Figs. 9 and 10; the rabbit data and also data from Nightingale et al. (1981) are included for comparison. No large differences are seen between the species. The data were analysed as before and, as expected, similar conclusions were obtained.

Electrical Properties of Developing Rabbit Brain

These experiments were undertaken to obtain data over a range of ages, such information being sparse in the literature. It is also of interest, however, to observe the dielectric behaviour of the water since we know that the water content of the brain decreases from birth to maturity.

Four rabbits from the same litter were systematically sacrificed (by cervical dislocation) at intervals over 23 days, the youngest being between 6 and 8 h old. Very little myelination was evident in the brain of the newly born animal, and the appearance of regions normally consisting of white matter (e.g., the brain stem and cerebral nucleus) was more in accord with that of grey matter. This was also observed for the 2-day-old animal.

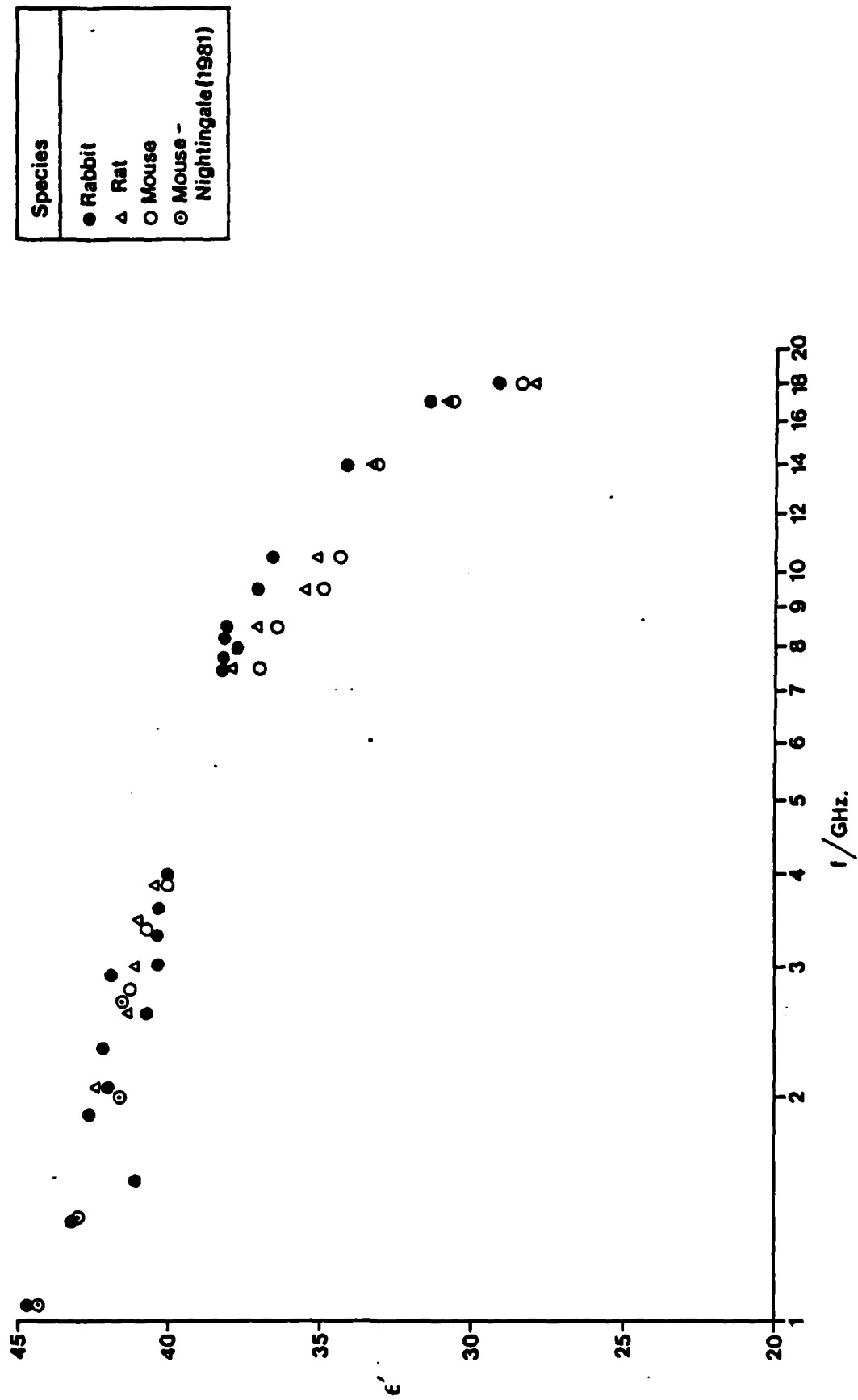


Figure 9. The permittivity of macerated brain tissue, showing various species at 37°C.

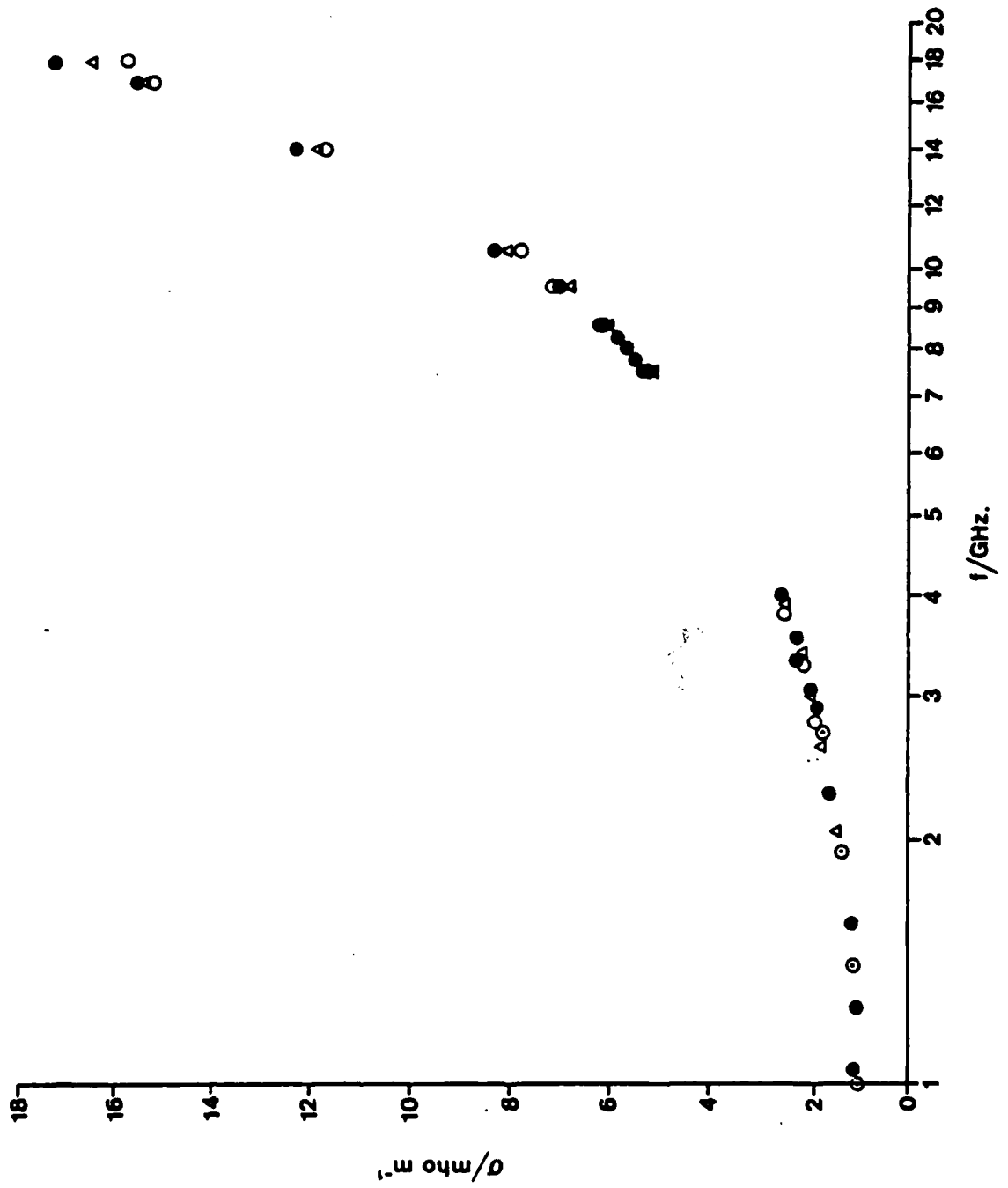


Figure 10. The conductivity of macerated brain tissue, showing various species at 37°C.

After 9 days, however, extensive myelination had taken place; and after 23 days the brain structure and size appeared similar to that of an adult rabbit.

The results are shown in Figs. 11 and 12 and are compared with those of the adult rabbit. That the youngest brains have the highest permittivity is to be expected, from the higher water content. The analysis of the data is given in Table 7, where only the 7.5- to 18-GHz data have been fitted to ensure that processes other than bulk water did not affect the results. In all cases the values of α were small and did not differ significantly from 0. Perhaps the most interesting result was that the static permittivity (ϵ_s) fell by 28% by the time the animals reached maturity, whereas the water content was only reduced by 10%. This decrease in ϵ_s is shown in Fig. 13 as a function of age, and the percentage change in ϵ_s as a function of percentage change of water content is shown in Fig. 14.

TABLE 7. DEVELOPING RABBIT BRAIN AT 37°C^a

Age	ϵ_s	f_R /GHz	α	σ_1 /mho m ⁻¹	RMSE
6-8 h	57.4 (1.1) ^b	26.1 (1.7)	-	1.45 (0.69)	0.593
	59.8 (2.9)	25.1 (2.0)	0.05 (0.05)	1.04 (0.78)	0.502
2 d	55.1 (1.4)	24.5 (1.8)	-	0.95 (0.80)	0.753
	57.4 (3.9)	23.7 (2.3)	0.05 (0.06)	0.60 (0.90)	0.692
9 d	52.2 (1.1)	26.7 (1.8)	-	1.44 (0.66)	0.652
	54.7 (3.1)	25.7 (2.2)	0.06 (0.06)	1.07 (0.75)	0.565
23 d	44.8 (1.0)	27.2 (2.1)	-	1.36 (0.63)	0.620
	47.7 (3.0)	25.7 (2.5)	0.08 (0.07)	0.91 (0.69)	0.501
Adult	40.6 (0.5)	28.2 (1.4)	-	1.41 (0.30)	0.403
	41.8 (1.4)	27.7 (1.5)	0.04 (0.04)	1.21 (0.35)	0.360

^aOnly data between 7.5 and 18 GHz have been used in the analysis.

^bThe errors are the 95% confidence intervals.

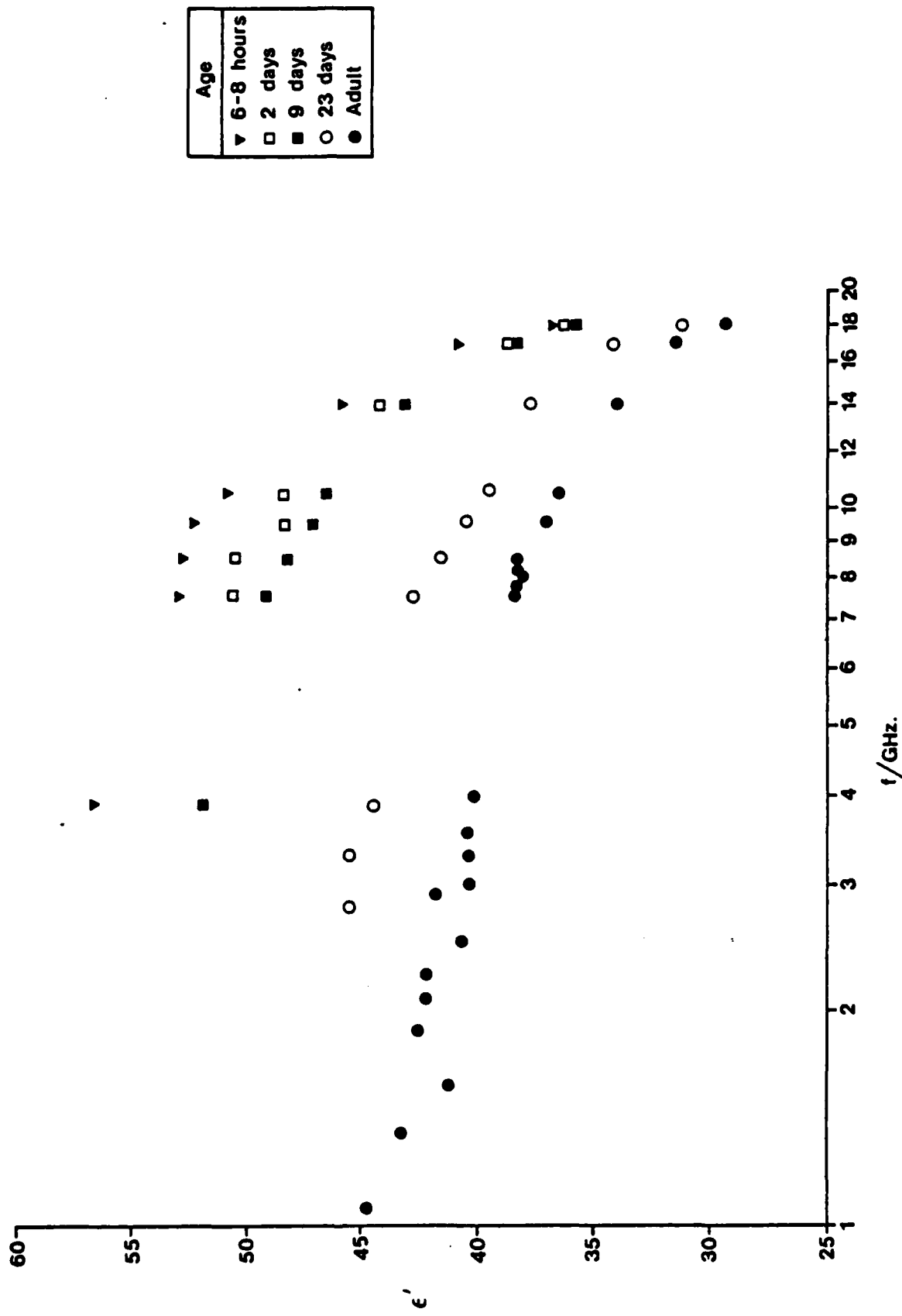


Figure 11. The permittivity of developing rabbit brain at 37°C.

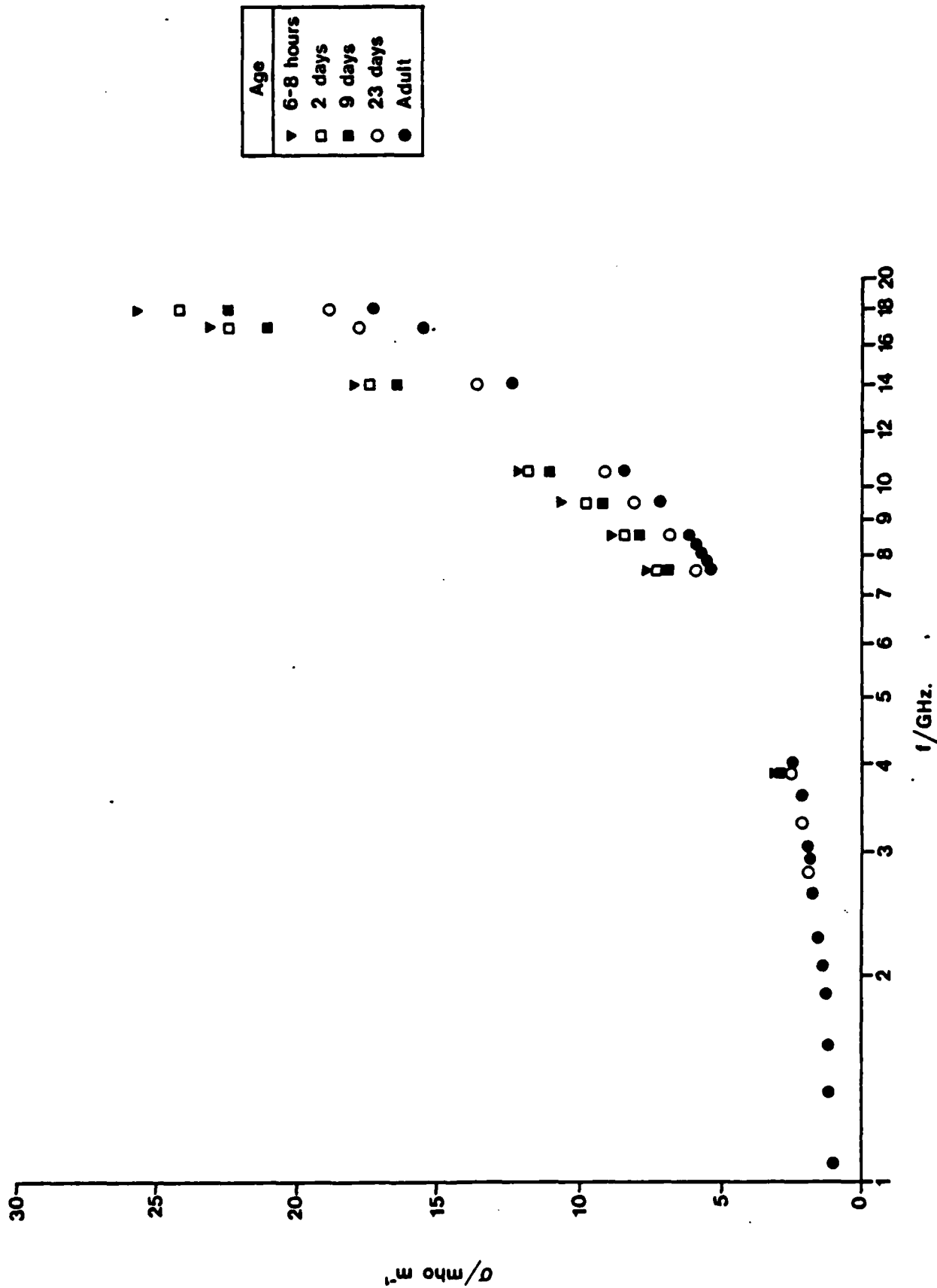


Figure 12. The conductivity of developing rabbit brain at 37°C.

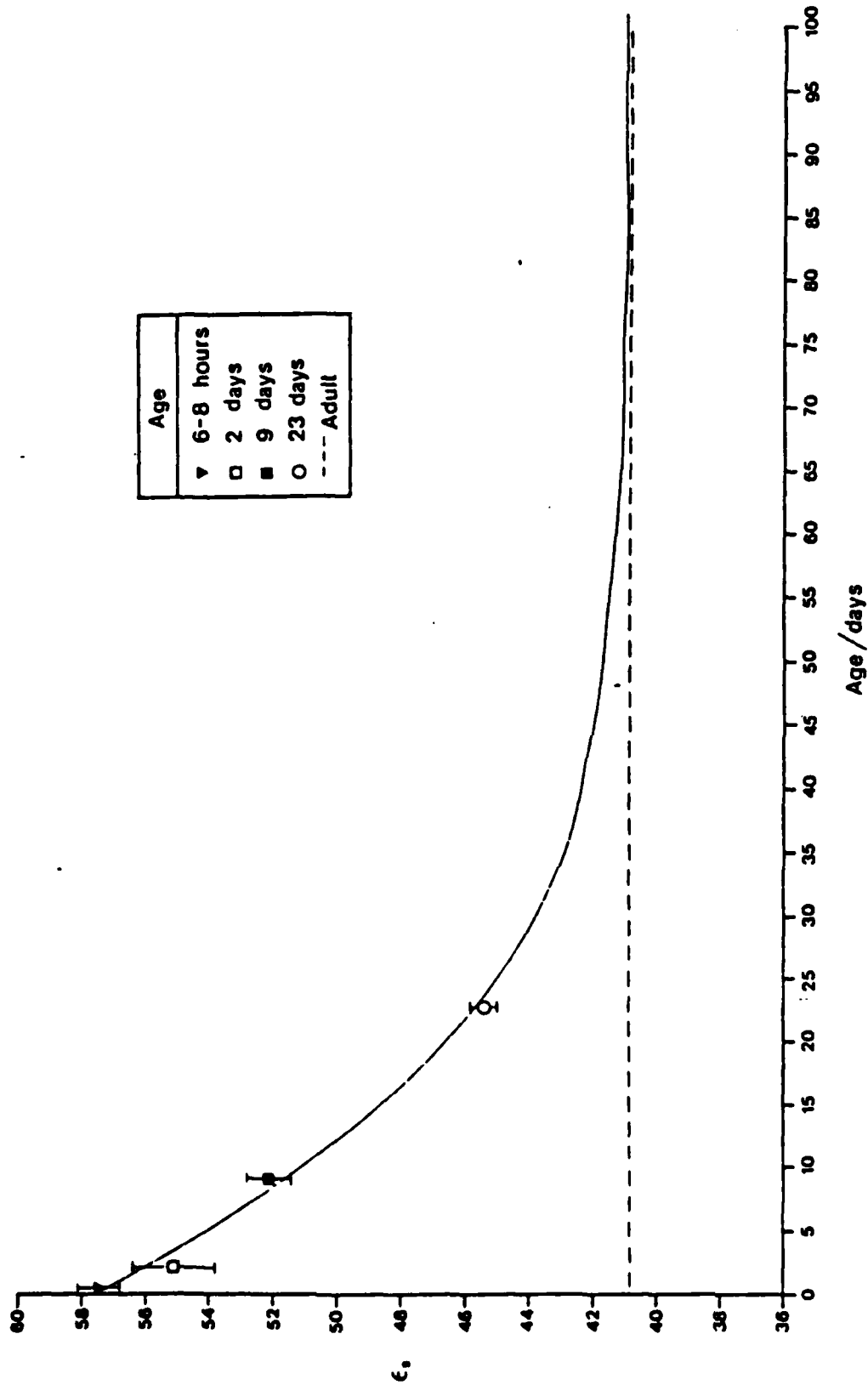


Figure 13. Microwave static permittivity (ϵ_s) v. age, for developing rabbit brain.

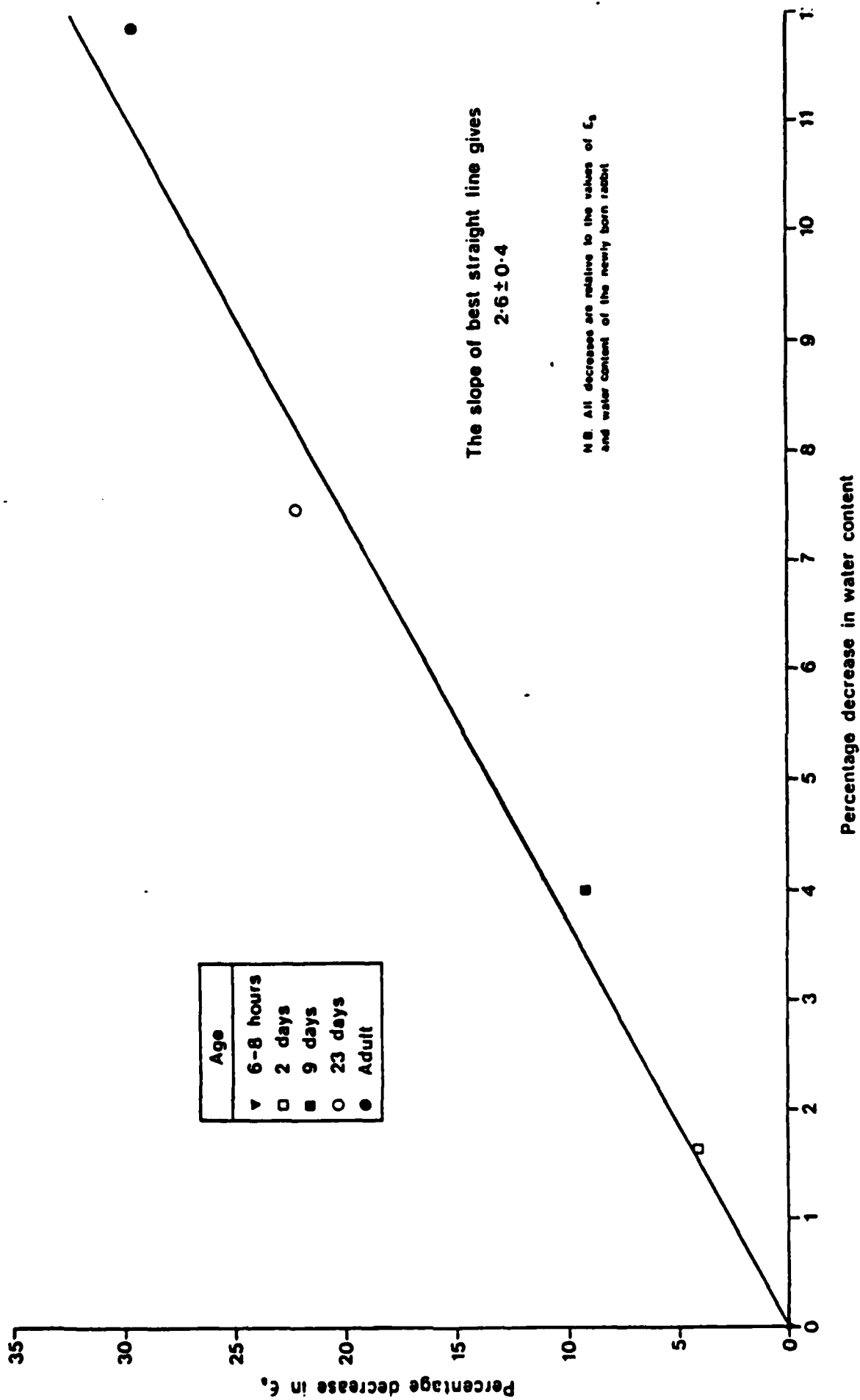


Figure 14. The decrease in microwave static permittivity (ϵ_s) v. decrease in water content during rabbit brain development.

Bound Water Estimation

The previous sections have shown that the bulk water in brain tissue behaves in a manner similar to free water in terms of its rotational mobility. However, the work has indicated that other processes relaxing at lower frequencies can affect the complex permittivity up to a few GHz. Gabriel (1983) has shown that for an intracellular component to contribute to the β dispersion above a few hundred MHz, it should have a radius less than 0.06 μm . Moreover such components, if present, would have a very small volume fraction. This, coupled with the small radius, would result in a negligibly small dielectric increment. Consequently it is likely that it is hydrated water which is relaxing between 0.1 and 1 GHz and thus contributing to the complex permittivity above 1 GHz.

In the following calculations the Maxwell-Fricke mixture theory is employed. Although specifically designed for simple systems, it approximates well to the situation pertaining in whole tissue. Moreover it has been used extensively by previous workers and should thus provide a useful comparison between bound water values, even if the absolute values must be treated with some reservation. This equation can be written as

$$\frac{\epsilon - \epsilon_1}{\epsilon + 2\epsilon_1} = v \frac{\epsilon_2 - \epsilon_1}{\epsilon_2 + 2\epsilon_1} \quad (9)$$

where ϵ is the permittivity of the mixture; ϵ_1 and ϵ_2 are the permittivities of the solvent and solute respectively; and v is the volume fraction of the hydrated solute.

With suitable values for these parameters (Steel 1984), the bound water values for the adult rabbit, the different species, and the developing brain are shown in Tables 8, 9, and 10. In all cases the bound water fraction is around 0.5 ml/ml of solid, which agrees well with the results of Foster et al. (1979) for canine brain.

TABLE 8. BOUND WATER IN ADULT RABBIT BRAIN

Tissue	T/°C	ϵ_s	Water fraction (volume basis)		Bound water fraction (ml/ml hydrated tissue)	
			Calculated	Measured	Value	Mean value
Macerated brain	20	40.5 (1.6) ^a	0.56 (0.02)		0.53 (0.06)	
				0.80 (0.02)		0.51 (0.05)
	37	40.6 (0.5)	0.61 (0.01)		0.48 (0.04)	
Grey matter	20	46.9 (1.9)	0.64 (0.02)		0.55 (0.09)	
				0.84 (0.02)		0.54 (0.06)
	37	45.0 (0.7)	0.67 (0.01)		0.52 (0.05)	
White matter	20	35.6 (1.6)	0.50 (0.02)		0.51 (0.06)	
				0.75 (0.02)		0.51 (0.06)
	37	33.6 (1.0)	0.51 (0.02)		0.50 (0.05)	

^aThe errors in brackets are the 95% confidence intervals.

TABLE 9. BOUND WATER IN BRAIN OF DIFFERENT SPECIES

Species	ϵ_s (at 37°C)	Water fraction (volume basis)		Bound water fraction (ml/ml hydrated tissue)	
		Calculated	Measured	Value	Mean value
Rabbit	40.6 (0.5) ^a	0.61 (0.01)	0.80 (0.02)	0.48 (0.04)	
Mouse	38.4 (0.8)	0.58 (0.01)	0.78 (0.02)	0.48 (0.05)	
Rat	39.5 (1.0)	0.59 (0.02)	0.81 (0.02)	0.54 (0.05)	

^aThe errors are the 95% confidence intervals.

TABLE 10. BOUND WATER IN DEVELOPING RABBIT BRAIN

Age	ϵ_s (at 37°C)	Water fraction (volume basis)		Bound water fraction (ml/ml hydrate tissue)	
		Calculated	Measured	Value	Mean value
6-8 h	57.5 (0.6) ^a	0.82 (0.01)	0.90 (0.01)	0.46 (0.07)	
2 d	55.1 (1.4)	0.79 (0.02)	0.89 (0.02)	0.47 (0.11)	
9 d	52.2 (0.7)	0.76 (0.01)	0.87 (0.02)	0.45 (0.07)	
23 d	45.3 (0.5)	0.66 (0.02)	0.84 (0.02)	0.53 (0.06)	
Adult	40.6 (0.5)	0.61 (0.01)	0.80 (0.02)	0.48 (0.04)	

^aErrors are the 95% confidence intervals.

RESULTS FOR RABBIT LENS

In view of the known connection between cataracts and microwave exposure, the measuring technique was used to determine the dielectric properties of lens material; in particular, to complement previous work (Dawkins et al. 1981, Gabriel et al. 1983) and to extend it to higher frequencies. The previous work had an upper frequency limit of 10 GHz.

Pigmented Dutch rabbits weighing more than 2.5 kg were used in this study. The eyes were excised within minutes of sacrifice and prepared as detailed by Steel (1984). The results for the permittivity and conductivity are shown in Figs. 15 and 16, which also give the low frequency data taken previously in this laboratory (Gabriel 1963, Gabriel et al. 1983).

There was good agreement between the data in the neighbourhood of 4 GHz where the results taken by the two different methods overlapped. The analysis of the lens cortex at 37°C is shown in Table 11; the data were analysed in various regions, as was done for the brain tissue. In the lens case however, the fitted parameters are independent of the data range chosen. This behaviour, contrasting to that of the brain material, indicates that there is only one dispersive process in the region of 1-18 GHz. The Cole-Cole model is a better fit than the Debye, and a significant value of α (in the range 0.10 to 0.13) is observed. The relaxation frequency is lower than for water, i.e. the fitted values are around 20 GHz as compared with 25.4 GHz.

An analysis of the lens nucleus is given in Table 12. Although similar results are obtained, the errors on α are larger, so the values are not significantly different from zero.

Results were also taken at 20°C (shown in Figs. 17 and 18, with the analysis in Tables 13 and 14) and the conclusions are in agreement with those at 37°C. The Maxwell-Fricke theory (Equation 9) was used to obtain values for the water of hydration (shown in Table 15).

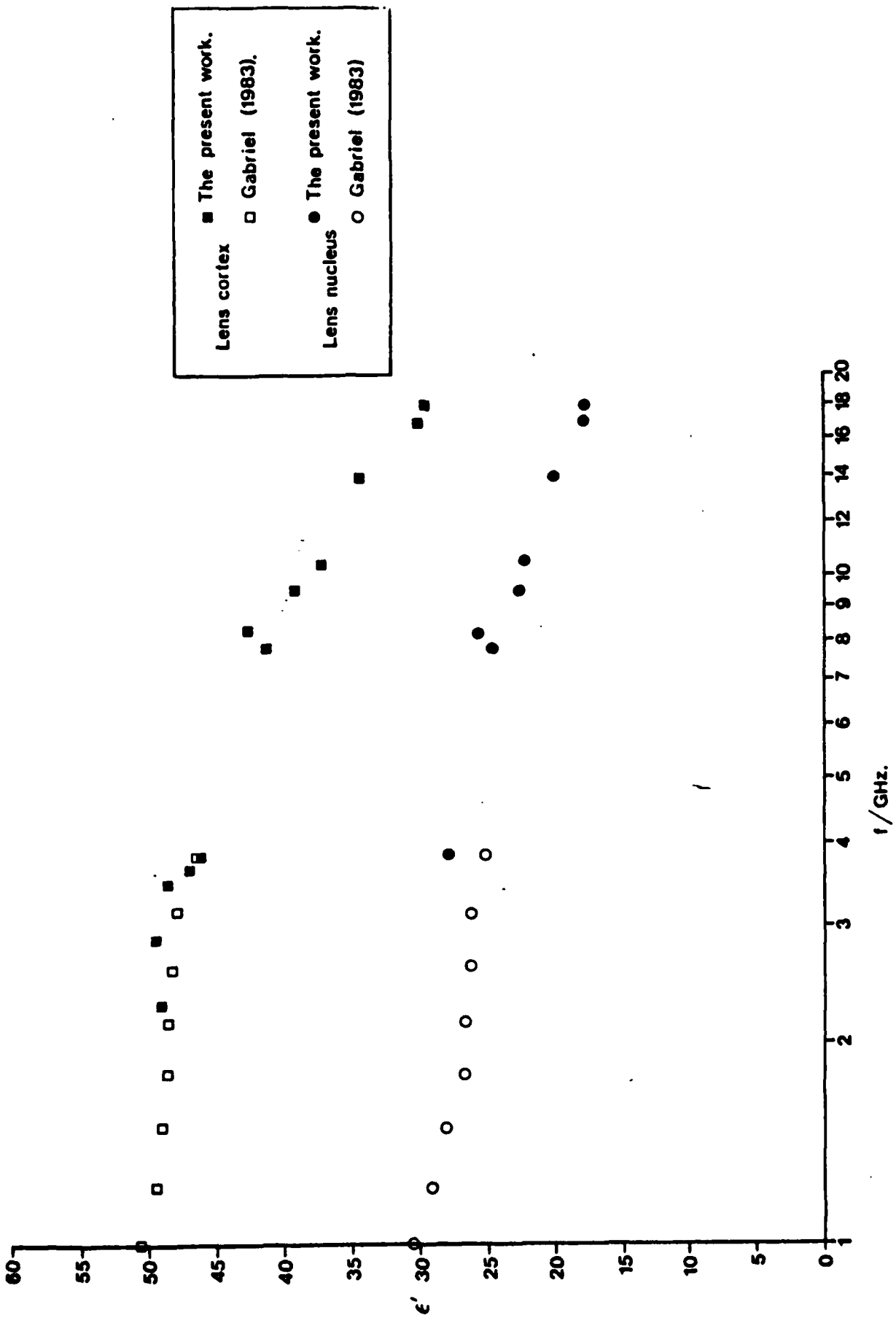


Figure 15. The permittivity of rabbit lens at 37°C.

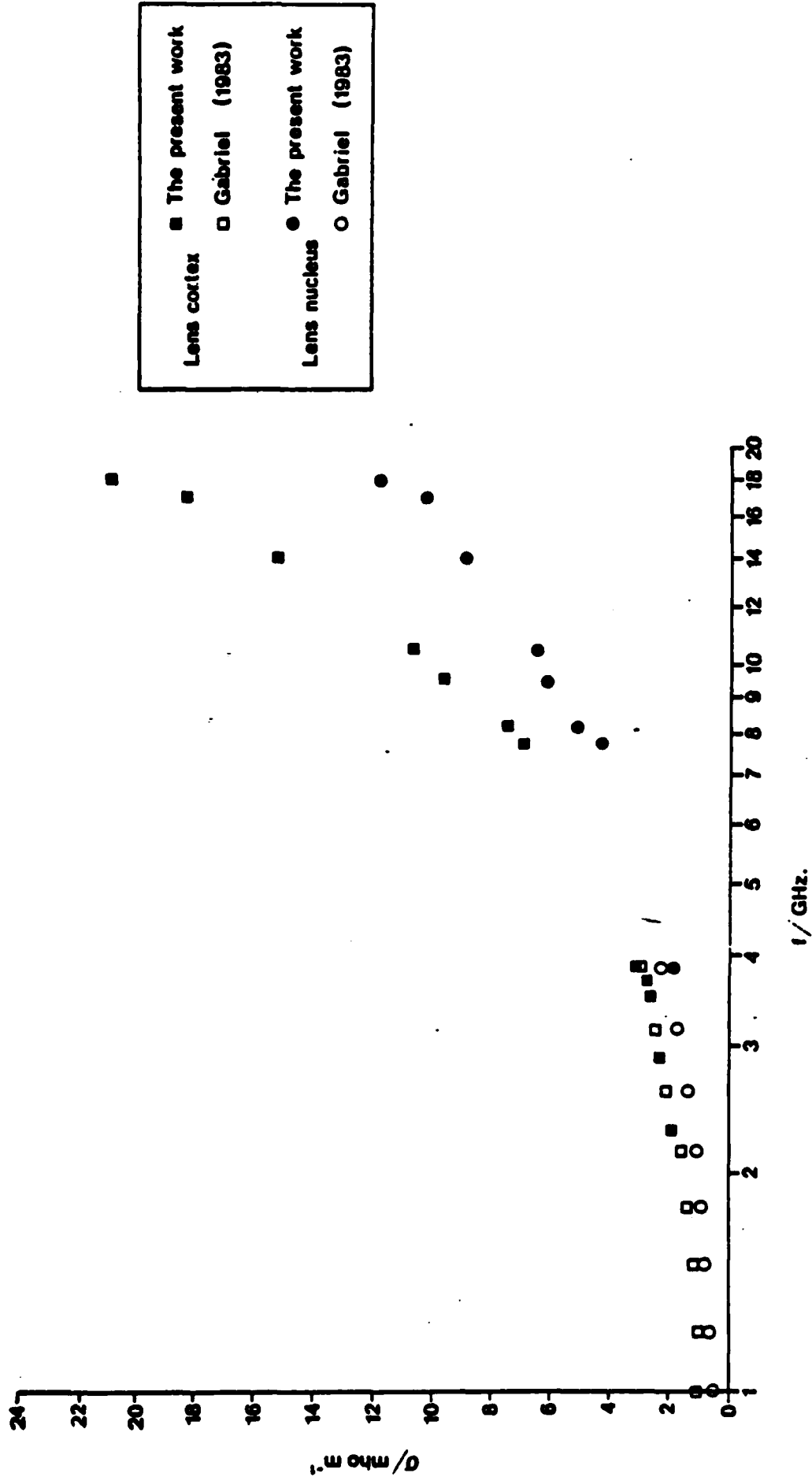


Figure 16. The conductivity of rabbit lens at 37°C.

TABLE 11. LENS CORTEX (RABBIT) AT 37°C

Range/GHz	N ^a	ϵ_s	f_R /GHz	α	σ_i /mho m ⁻¹	RMSE
1-18 ^b	42	51.1 (0.7) ^c	19.3 (0.7)	0.12 (0.03)	0.83 (0.05)	0.679
		48.7 (0.6)	19.4 (1.0)	-	0.94 (0.08)	1.263
1-10.5 ^b	36	51.3 (0.9)	19.1 (1.0)	0.13 (0.04)	0.82 (0.06)	0.688
		49.0 (0.6)	18.2 (1.0)	-	0.91 (0.07)	1.079
2.3-18	24	51.3 (1.3)	19.7 (1.0)	0.12 (0.03)	0.92 (0.14)	0.649
		47.7 (1.5)	20.8 (1.4)	-	1.20 (0.20)	1.253
7.8-18	14	51.1 (4.0)	19.2 (2.4)	0.10 (0.06)	0.46 (0.82)	0.501
		45.8 (1.5)	21.9 (1.9)	-	1.26 (0.81)	0.726

^aThe number of real and imaginary data points used in the analysis.

^bDenotes that data from Gabriel (1983) have been used in addition to the data obtained from the present work.

^cThe errors are the 95% confidence intervals.

$$(\epsilon_\infty = 5.1)$$

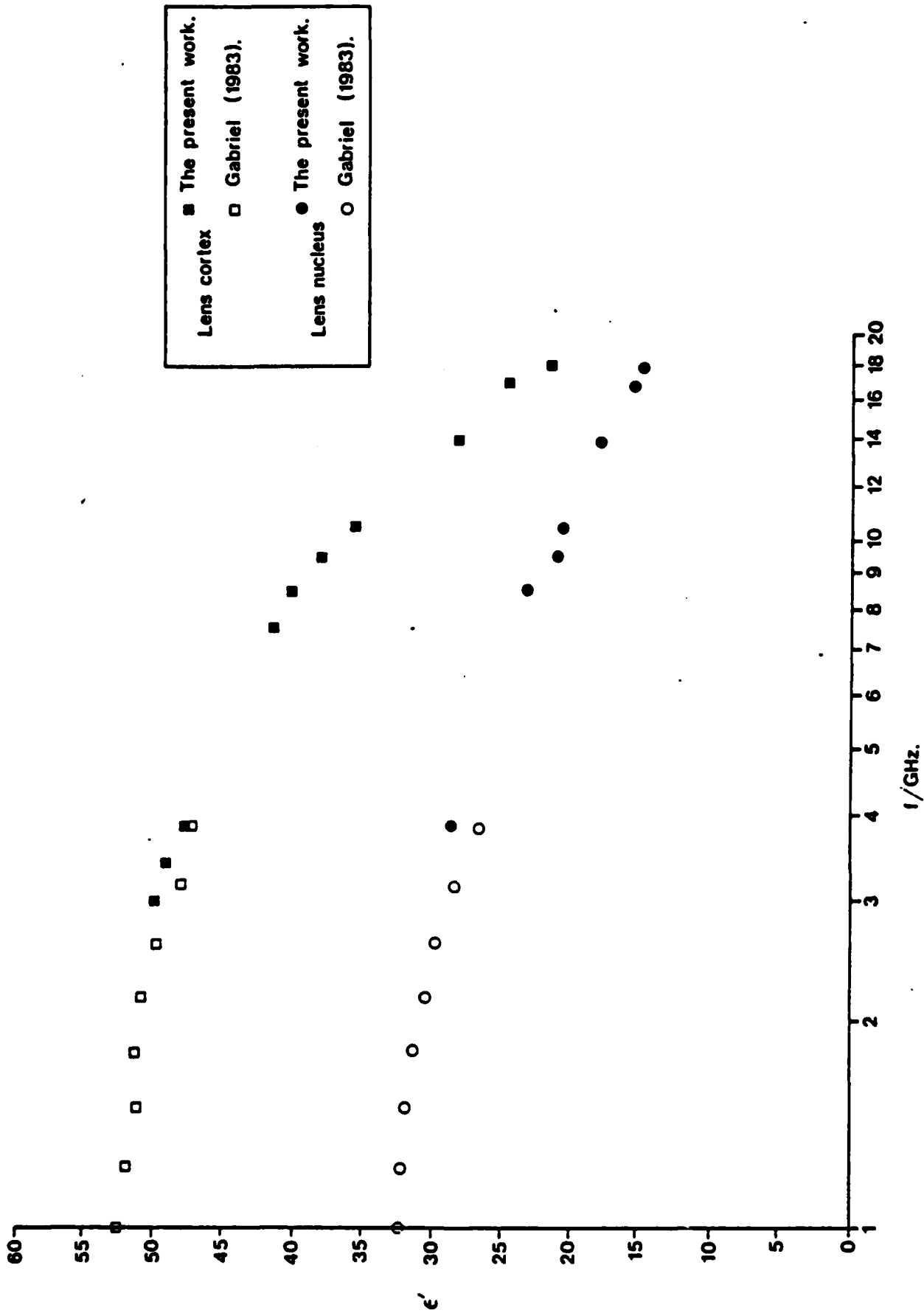


Figure 17. The permittivity of rabbit lens at 20°C.

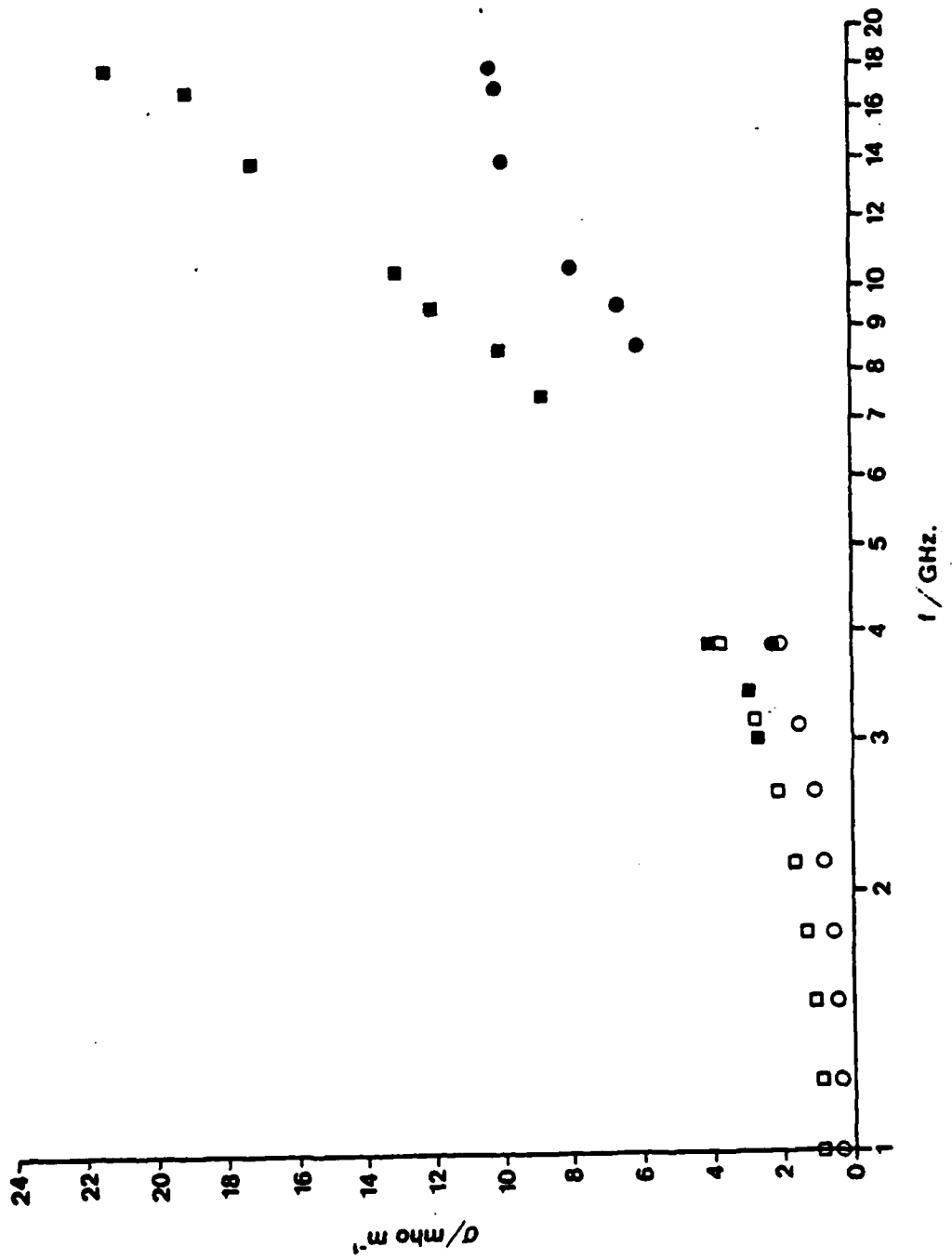


Figure 18. The conductivity of rabbit lens at 20°C.

TABLE 12. LENS NUCLEUS (RABBIT) AT 37°C

Range/GHz	N ^a	ϵ_s	f_R /GHz	α	σ_1 /mho m ⁻¹	RMSE
1-18 ^b	34	29.2 (1.6) ^c	16.5 (2.3)	0.09 (0.10)	0.60 (0.11)	1.474
		28.1 (0.9)	17.0 (2.1)	-	0.64 (0.11)	1.554
1-10.5 ^b	28	29.0 (1.9)	15.0 (2.6)	0.07 (0.14)	0.58 (0.12)	1.524
		28.3 (1.0)	15.0 (2.3)	-	0.61 (0.11)	1.550
3.85-18	16	30.5 (2.6)	17.3 (2.6)	0.10 (0.08)	0.70 (0.40)	0.605
		27.9 (1.0)	19.1 (1.9)	-	0.90 (0.40)	0.749

^aThe number of real and imaginary data points used in the analysis.

^bDenotes that data from Gabriel (1983) have been used in addition to the data obtained from the present work.

^cThe errors are the 95% confidence intervals.

($\epsilon_\infty = 5.1$)

TABLE 13. LENS CORTEX (RABBIT) AT 20°C

Range/GHz	N ^a	ϵ_s	f_R /GHz	α	σ_I /mho m ⁻¹	RMSE
1-18 ^b	38	53.3 (1.1) ^c	13.2 (0.6)	0.07 (0.03)	0.63 (0.08)	1.068
		51.5 (0.8)	13.7 (0.7)	-	0.71 (0.09)	1.342
1-10.5 ^b	32	53.2 (1.3)	13.7 (0.8)	0.07 (0.04)	0.65 (0.09)	1.042
		51.7 (0.7)	13.8 (0.8)	-	0.71 (0.09)	1.198
3-18	20	53.7 (3.0)	13.5 (1.3)	0.07 (0.05)	0.82 (0.37)	1.111
		50.5 (1.5)	14.4 (1.0)	-	1.04 (0.40)	1.330
7.6-18	14	59.3 (17.9)	11.6 (5.3)	0.11 (0.13)	0.01 (2.60)	1.083
		52.1 (4.2)	13.7 (1.7)	-	0.01 (1.50)	1.123

^aThe number of real and imaginary data points used in the analysis.

^bDenotes that data from Gabriel (1983) have been used in addition to the data obtained from the present work.

^cThe errors are the 95% confidence intervals.

($\epsilon_m = 5.5$)

TABLE 14. LENS NUCLEUS (RABBIT) AT 20°C

Range/GHz	N ^a	ϵ_s	f_R /GHz	α	σ_1 /mho m ⁻¹	RMSE
1-18 ^b	32	33.4 (1.2) ^c	10.9 (1.0)	0.13 (0.05)	0.26 (0.07)	0.831
		31.1 (0.8)	12.0 (1.0)	-	0.35 (0.08)	1.197
1-10.5 ^b	26	33.3 (1.4)	10.6 (1.1)	0.12 (0.07)	0.25 (0.08)	0.847
		31.4 (0.7)	11.2 (1.0)	-	0.32 (0.08)	1.059
3.85-18	14	34.3 (4.1)	11.0 (2.4)	0.13 (0.07)	0.42 (0.45)	0.592
		29.2 (1.8)	13.9 (1.7)	-	0.80 (0.50)	0.908

^aThe number of real and imaginary data points used in the analysis.

^bDenotes that data from Gabriel (1983) have been used in addition to the data obtained from the present work.

^cThe errors are the 95% confidence intervals.

$$(\epsilon_\infty = 5.5)$$

TABLE 15. BOUND WATER IN RABBIT LENS

Tissue T/°C	ϵ_s	Water fraction (volume basis)		Bound water fraction (ml/ml hydrated tissue)	
		Calculated	Measured	Value	Mean value
Cortex:					
20	53.3 (1.1) ^a	0.72 (0.01)		0.17 (0.09)	
			0.77 (0.02)		0.14 (0.09)
37	51.1 (0.7)	0.74 (0.01)		0.10 (0.09)	
Nucleus:					
20	33.4 (1.2)	0.46 (0.02)		0.29 (0.07)	
			0.62 (0.04)		0.31 (0.08)
37	29.2 (1.6)	0.44 (0.03)		0.32 (0.08)	

^a The errors are the 95% confidence intervals.

CONCLUSIONS

The principal objective of this research was to devise a technique to measure accurately the electrical properties of solid biological tissue in the frequency range 1-18 GHz. The measuring technique evolved to fulfill this aim is based on the original Roberts-Von Hippel method but modified such that the standing wave produced by the sample is recorded onto a floppy disc and the complete waveform is analysed by a microcomputer. This method measured the relative permittivity and dielectric loss of typical solid tissues to within $\pm 1\%$ and $\pm 2\%$ respectively (these errors corresponding to the standard deviation in the measured parameter). For substances such as pure water, where there is no biological variation between samples, the errors are halved.

The equipment was used to determine the dielectric properties of lens material and brain tissue in the designated frequency range. The dielectric properties of the bulk water in the two tissues were markedly different, with a much higher proportion of the bulk water in brain behaving similarly to pure water. This is consistent with what is known about the differences in structure between the tissues. In the brain tissue the nonaqueous components are relatively concentrated into localised regions, whereas in lens materials the biological macromolecules are more uniformly distributed.

REFERENCES

1. Burdette, E.C.; Cain, F.L.; and Seals, J. 1980. In vivo probe measurement technique for determining dielectric properties at UHF through microwave frequencies. IEEE Trans Microwave Theory Tech, MTT-28 414-427.
2. Dawkins, A.W.J.; Sheppard, R.J.; and Grant, E.H. 1979. An on-line computer-based system for performing a time domain spectroscopy. I: Description of the main features of the basic system. J Phys E Sci Instrum 12, 1091-1099.
3. Dawkins, A.W.J.; Gabriel, C.; Sheppard, R.J.; and Grant, E.H. 1981. Electrical properties of lens material at microwave frequencies. Phys Med Biol 26, 1-9.
4. Foster, K.R.; Schepps, J.L.; Stoy, R.D.; and Schwan, H.P. 1979. Dielectric properties of brain tissue between 0.01 and 10 GHz. Phys Med Biol 24, 1177-1187.
5. Foster, K.R.; Schepps, J.L.; and Schwan, H.P. 1980. Microwave dielectric relaxation in muscle: A second look. Biophys J 29, 271-281.
6. Gabriel, C.H.B. 1983. Dielectric study of ocular tissue using time domain spectroscopy. Ph.D. Thesis, University of London.
7. Gabriel, C.; Sheppard, R.J.; and Grant, E.H. 1983. Dielectric properties of ocular tissues at 37°C. Phys Med Biol 28, 43-49.
8. Grant, E.H.; Sheppard, R.J.; and South, G.P. 1978. Dielectric Behaviour of Biological Molecules in Solution. New York: Oxford University Press.
9. Nightingale, N.R.V.; Szwarnowski, S.; Sheppard, R.J.; and Grant, E.H. 1981. A coaxial line cell for measuring the permittivity of medium to high loss liquids in the frequency range 2-15 GHz. J Phys E Sci Instrum 14, 156-160.
10. Nightingale, N.R.V.; Goodridge, V.D.; Sheppard, R.J.; and Christie, J.L. 1983. The dielectric properties of the cerebellum, cerebrum, and brain stem of mouse brain at radiowave and microwave frequencies. Phys Med Biol 28, 897-903.
11. Roberts, S.; and Von Hippel, A. 1946. A new method for measuring the dielectric constant and loss in the range of centimeter waves. J Appl Phys 17, 610-616.
12. Schepps, J.L.; and Foster, K.R. 1980. The UHF and microwave dielectric properties of normal and tumour tissues: variation in dielectric properties with tissue water content. Phys Med Biol 25, 1149-1159.

13. Sheppard, R.J. 1972. An automated coaxial line system for determining the permittivity of a liquid. *J Phys D Appl Phys* 5, 1576-1587.
14. Sheppard, R.J. 1973. The least-squares analysis of complex weighted data with dielectric applications. *J Phys D Apply Phys* 6, 790-794.
15. Sheppard, R.J.; and Grant, E.H. 1972. Design and construction of a coaxial line cell for measuring the complex permittivity of a liquid. *J Phys E Sci Instrum* 5, 1208-1212.
16. Steel, M.C. 1984. The development of a frequency domain technique to measure the complex permittivity of biological tissues in vitro from 1 to 18 GHz. Ph.D: Thesis, University of London.
17. Steel, M.C.; Sheppard, R.J.; and Grant, E.H. 1984. A precision method for measuring the complex permittivity of solid tissue in the frequency domain between 2 and 18 GHz. *J Phys E Sci Instrum* 17, 30-34.
18. Stuchly, M.A.; Athey, T.W.; Stuchly, S.S.; Samaras, G.M.; and Taylor, G.E. 1981. Dielectric properties of animal tissues in vivo at frequencies 10 MHz-1 GHz. *Bioelectromagnetics* 2, 93-103.
19. Stuchly, M.A.; Athey, T.W.; Samaras, G.M.; and Taylor, G.E. 1982a. Measurement of radiofrequency permittivity of biological tissues with an open-ended coaxial line. Part II: Experimental results. *IEEE Trans Microwave Theory Tech*, MTT-30, 87-92.
20. Stuchly, M.A.; Kraszewski, A.; Stuchly, S.S.; and Smithie, A.M. 1982b. Dielectric properties of animal tissues in vivo at radio and microwave frequencies. *Phys Med Biol* 27, 927-936.
21. Szwarnowski, S.; and Sheppard, R.J. 1977. Precision waveguide cells for the measurement of permittivity of lossy liquids at 70 GHz. *J Phys E Sci Instrum* 10, 1163-1167.

END

11 - 86

DTIC